THE JOURNAL OF BIOLOGICAL CHEMISTRY VOL. 289, NO. 18, pp. 12550–12565, May 2, 2014
Published in the U.S.A.

Long Non-coding RNA *HOTAIR* Is Targeted and Regulated by miR-141 in Human Cancer Cells*

Received for publication, October 9, 2013, and in revised form, February 26, 2014 Published, JBC Papers in Press, March 10, 2014, DOI 10.1074/jbc.M113.488593

Takeshi Chiyomaru[‡], Shinichiro Fukuhara[‡], Sharanjot Saini[‡], Shahana Majid[‡], Guoren Deng[‡], Varahram Shahryari[‡], Inik Chang[§], Yuichiro Tanaka[‡], Hideki Enokida[¶], Masayuki Nakagawa[¶], Rajvir Dahiya[‡], and Soichiro Yamamura[‡]

From the [‡]Department of Urology, San Francisco Veterans Affairs Medical Center and University of California, San Francisco, San Francisco, California 94121, the [§]Department of Oral Biology, College of Dentistry, Yonsei University, Seoul 120-752, Korea, and the [¶]Department of Urology, Graduate School of Medical and Dental Sciences, Kagoshima University, Kagoshima 890-8520, Japan

Background: Silencing of long non-coding RNA (lncRNA) by microRNA (miRNA) has only been recently observed.
Results: miR-141 binds to *HOTAIR* and suppresses its oncogenic function in Ago2 (Argounaute2).
Conclusion: miR-141 targets and silences *HOTAIR* in an Ago2-dependent manner in cancer cells.
Significance: Our results suggest that regulation of lncRNA expression by miRNA plays essential roles in gene expression and cellular functions.

***HOTAIR* is a long non-coding RNA that interacts with the polycomb repressive complex and suppresses its target genes. *HOTAIR* has also been demonstrated to promote malignancy. MicroRNA-141 (miR-141) has been reported to play a role in the epithelial to mesenchymal transition process, and the expression of miR-141 is inversely correlated with tumorigenicity and invasiveness in several human cancers. We found that *HOTAIR* expression is inversely correlated to miR-141 expression in renal carcinoma cells. *HOTAIR* promotes malignancy, including proliferation and invasion, whereas miR-141 suppresses malignancy in human cancer cells. miR-141 binds to *HOTAIR* in a sequence-specific manner and suppresses *HOTAIR* expression and functions, including proliferation and invasion. Both *HOTAIR* and miR-141 were associated with the immunoprecipitated Ago2 (Argonaute2) complex, and the Ago2 complex cleaved *HOTAIR* in the presence of miR-141. These results demonstrate that *HOTAIR* is suppressed by miR-141 in an Ago2-dependent manner.**

Non-coding RNAs have been demonstrated to have important roles in gene regulation, and a large number of long non-coding RNAs (lncRNAs)[2] have been discovered (1–3). lncRNAs are differentially expressed in various tissues and have important functions in gene regulation in normal and cancer cells (4–6). lncRNAs function through diverse molecular mechanisms (7), and a number of lncRNAs associate with chromatin-modifying complexes affecting gene expression (8–12). *HOTAIR* is an lncRNA localized in the *HOXC* gene cluster, and it interacts with PRC2 (polycomb repressive complex 2), which enhances H3K27 trimethylation to decrease expression of multiple genes (13). *HOTAIR* expression has been shown to promote cancer cell invasiveness (13, 14) and to increase proliferation, cell cycle progression, and reduced apoptosis (15).

MicroRNAs (miRNAs) are highly conserved, single-stranded, non-coding RNAs of ~21–24 nucleotides that regulate gene expression by posttranscriptional silencing of specific target RNAs. They repress translation or cleave RNA transcripts by binding to the 3′-untranslated region (3′-UTR) of target messenger RNAs (mRNAs) (16–19). Therefore, miRNAs regulate diverse cellular processes, such as cell cycle progression, proliferation, apoptosis, development, and function as oncogenes or tumor suppressor genes (20, 21). The miRNA-200 family (miR-200a, miR-200b, miR-200c, miR-141, and miR-429) was previously shown to inhibit ZEB1, up-regulate E-cadherin, and reduce cell motility, indicating that the miRNA-200 family plays a role in the epithelial to mesenchymal transition process (22–26). The expression of miR-141 is inversely correlated with tumorigenicity and invasiveness in several human cancers.

Here we show that *HOTAIR* promotes malignancy, including proliferation and invasion, whereas miR-141 suppresses malignancy in cancer cells. miR-141 was found to bind *HOTAIR* in a sequence-specific manner and suppress *HOTAIR* expression and function, including proliferation and invasion, in cancer cells. Suppression of *HOTAIR* expression by miR-141 correlated with alteration of *HOTAIR* function. miR-141 suppression of *HOTAIR* expression was found to be Ago2 (Argonaute2)-dependent. Immunoprecipitation studies showed that *HOTAIR* was pulled down with miR-141 in the Ago2 complex, and *HOTAIR* was cleaved by Ago2 in the presence of miR-141. Our results demonstrate that *HOTAIR* is suppressed by miR-141 in an Ago2-dependent manner.

EXPERIMENTAL PROCEDURES

Cell Culture and Transfection—Human renal carcinoma cells (786-O and ACHN cells), prostate cancer cells (DU145), colorectal adenocarcinoma cells (HT-29 cells), and normal HK-2 kidney cells were purchased from the American Type

* This work was supported, in whole or in part, by National Institutes of Health Grant RO1CA130860. This study was also supported by Veterans Affairs Program Project and Veterans Affairs Merit Review grants.
[1] To whom correspondence should be addressed: Urology Research Center (112F), Veterans Affairs Medical Center and University of California, San Francisco, 4150 Clement St., San Francisco, CA 94121. Tel.: 415-221-4810; Fax: 415-750-6645; E-mail: yamamuras@urology.ucsf.edu.
[2] The abbreviations used are: lncRNA, long intergenic non-coding RNA; miRNA, microRNA; 7-AAD, 7-aminoactinomycin D.

Culture Collection (Manassas, VA). 786-O cells were cultured in RPMI 1640 medium supplemented with 10% fetal bovine serum (FBS). ACHN and DU145 cells were cultured in Eagle's minimum essential medium supplemented with 10% FBS. HT-29 cells were cultured in McCoy's 5A medium supplemented with 10% FBS. HK-2 cells were cultured in keratinocyte serum-free medium (Invitrogen) with bovine pituitary extract and human recombinant epidermal growth factor (EGF). α-Amanitin was purchased from Sigma-Aldrich. α-Amanitin was dissolved in water and added to 786-O and ACHN cells at a final concentration of 5 μg/ml.

Cells were transfected with either 30 nM pre-miR negative control or pre-miR-141 (Applied Biosystems, Foster City, CA) or 30 nM siRNA control or *HOTAIR* siRNA (Sigma-Aldrich) using Lipofectamine 2000 (Invitrogen), according to the manufacturer's instructions.

For co-transfection, cells were initially transfected with 20 nM pre-miR negative control or pre-miR-141 (Applied Biosystems) using Lipofectamine 2000 (Invitrogen), according to the manufacturer's instructions. Subsequently, the cells were transfected with 20 nM siRNA control or *HOTAIR* siRNA using Lipofectamine 2000, according to the manufacturer's instructions.

Subconfluent cells (60–70% confluent) were treated with 25 μM genistein (Sigma-Aldrich) dissolved in dimethyl sulfoxide, and cells treated only with dimethyl sulfoxide served as control. Cell media and genistein were changed every day, and cells were cultured for 4 days.

Cell Viability and Proliferation Assays—Cell viability was measured using the CellTiter 96 Aqueous One Solution cell proliferation assay (MTS assay) (Promega, Madison, WI), a colorimetric assay that measures the activity of reductase enzymes. Cells were seeded at a density of 1.5×10^3 cells/well in flat bottomed 96-well plates. At the indicated times, CellTiter 96 Aqueous One reagent was added to each well according to the manufacturer's instructions. Cell viability was determined by measuring the absorbance at 490 nm using a kinetic microplate reader (Spectra MAX 190; Molecular Devices Co., Sunnyvale, CA). A bromodeoxyuridine (BrdU) cell proliferation assay was performed using a BrdU cell proliferation kit (Millipore, Billerica, MA) according to the manufacturer's instructions. BrdU was incorporated into cells for 4 h, and the cells were fixed at the indicated times after transfection. Data are the mean ± S.D. of three independent experiments.

Apoptosis Analysis—Apoptosis was measured using flow cytometry (Cell Lab Quanta SC, Beckman Coulter, Brea, CA) with Annexin-V-FITC/7-AAD labeling. Measurements were repeated independently three times.

Transwell Invasion Assay—Culture inserts of 8-μm pore size (Transwell; Costar) were coated with Matrigel (BD Biosciences) (100 μg/well) and placed into the wells of 24-well culture plates. In the lower chamber, 500 μl of DMEM containing 10% FBS was added, and 1×10^5 cells were seeded to the upper chamber. After 36 h of incubation at 37 °C with 5% CO_2, the number of cells that had migrated through the pores were fixed with 10% formalin and stained with 0.05% crystal violet. Crystal violet was solubilized with methanol, and absorbance at 540 nm was measured by a kinetic microplate reader (Spectra MAX 190; Molecular Devices). Data are the mean ± S.D. of three independent experiments.

RNA Extraction and Quantitative Real-time PCR—Total RNA was isolated using the miRNeasy minikit (Qiagen, Valencia, CA) according to the manufacturer's instructions. Reverse transcription reactions were performed using the iScript cDNA synthesis kit (Bio-Rad) or reverse transcription system kit (Applied Biosystems). Quantitative real-time PCR analysis was performed in triplicate with an Applied Biosystems Prism7500 fast sequence detection system using TaqMan universal PCR master mix according to the manufacturer's protocol (Applied Biosystems). Levels of RNA expression were determined using the 7500 Fast System SDS software version 1.3.1 (Applied Biosystems).

Plasmids—A putative *HOTAIR* target site was cloned into the PmeI-XbaI site of the dual luciferase pmirGLO plasmid (Promega). For mismatch constructs, eight mismatches, which are shown in *boldface letters* in the *HOTAIR* sequence, AAACAGAGT**CC**GTT**CAGTGT**CA, in Fig. 4 were introduced in the putative target site, and the target site sequence was changed to AAACAGAGT**AA**GTT**AGTGAC**CA. The *HOTAIR* cDNA was amplified from cDNA of 786-O cells by using primers carrying BamHI and XhoI restriction enzyme sites at the flanking ends. The amplified cDNA was sequenced and subcloned into the BamHI and XhoI restriction site of the pcDNA3.1(+) plasmid (Invitrogen). A mutant *HOTAIR* expression plasmid was constructed with the eight mismatches in the sequence in the putative target site of *HOTAIR* in pmirGLO plasmid shown above by site-directed mutagenesis. Ago2 expression plasmid (pFRT/FLAG/HA-DEST-EIF2C2 (plasmid 19888)) (27) was purchased from Addgene (Cambridge, MA). A *HOTAIR* promoter region (−35 to −2286) (28) was cloned into the MluI-XhoI site of the pLightSwitch_Prom plasmid (SwitchGear Genomics, Carlsbad, CA).

Western Blot Analysis—Protein extracts were resolved by SDS-PAGE and transferred to polyvinylidene difluoride membranes (Hybond-P, GE Healthcare), followed by incubation with the indicated primary and secondary antibodies conjugated to horseradish peroxidase (GE Healthcare). Signals were detected using the ECL detection system (Amersham Biosciences ECL Plus Western blotting detection system). Antibodies against Ago2, ZEB1, E-cadherin, vimemtin, and GAPDH were purchased from Cell Signaling Technology (Danvers, MA). Antibodies against FLAG and fibronectin were purchased from Sigma-Aldrich or Abcam (Cambridge, MA), respectively. An antibody against RNA polymerase II was purchased from Millipore.

Luciferase Reporter Assay—Cells in 24-well plates were transfected with 30 nM pre-miR negative control or pre-miR-141 (Applied Biosystems) using Lipofectamin 2000 (Invitrogen), according to the manufacturer's instructions. Dual luciferase pmirGLO plasmid (Promega) was transfected using X-tremeGENE HP (Roche Applied Science) according to the manufacturer's instructions. Luciferase activity was assayed 48 h after transfection, using a Dual-Luciferase reporter assay system (Promega). The values were normalized to those obtained for pre-miR negative control transfection. All transfection experiments were performed in triplicate.

Cells in 24-well plates were transfected with 30 or 6 nM pre-miR negative control or pre-miR-141 (Applied Biosystems) using Lipofectamin 2000 (Invitrogen), according to the manufacturer's instructions. pLightSwitch_Prom plasmid harboring A *HOTAIR* promoter region or pLightSwitch_Prom plasmid only was transfected using X-tremeGENE HP (Roche Applied Science) according to the manufacturer's instructions. Luciferase activity was assayed 48 h after transfection, according to the manufacturer's instructions. All transfection experiments were performed in triplicate.

RNA Immunoprecipitation—786-O was transfected with FLAG-tagged Ago2 expression plasmid, *HOTAIR* expression plasmid, and pre-miR-141. RNA immunoprecipitation was performed using the Imprint RNA immunoprecipitation kit (Sigma-Aldrich). Anti-FLAG antibody (Sigma-Aldrich) and Protein G-agarose (Santa Cruz Biotechnology, Inc.) were used. Reverse transcription reactions were performed using iScript (Bio-Rad) and reverse transcription system kit (Applied Biosystems) *HOTAIR* and miR-141, respectively. Quantitative real-time PCR analysis was performed as described above.

HOTAIR Cleavage Assay—*HOTAIR* was *in vitro* transcribed using the RiboMAX^{TM} large scale RNA production system (Promega) with digoxigenin (DIG)-labeled UTP (Roche Applied Science) using the *HOTAIR* expression plasmid (pcDNA3.1(+)-*HOTAIR*) and was purified using RNAeasy (Qiagen). The immunoaffinity-purified Ago2 complexes were resuspended in 20 μl of buffer containing 100 mM KCl, 2 mM $MgCl_2$, and 10 mM Tris, pH 7.5, 8 units of RNAsin (Promega), and *HOTAIR*. After 2 h of incubation at 30 °C, RNA was isolated using the miRNeasy minikit (Qiagen). After Northern blotting, DIG was probed with a DIG nucleic acid detection kit (Roche Applied Science).

Statistical Analysis—Data are shown as mean values ± S.D. Student's *t* test was used to compare two different groups. *p* values of less than 0.05 were regarded as statistically significant ($n = 3$) and denoted with an asterisk, compared with control unless otherwise specified.

RESULTS

Inverse Expression of HOTAIR and miR-141 in Renal Carcinoma Cells—Real-time RT-PCR revealed that the expression level of *HOTAIR* was markedly higher in 786-O and ACHN compared with non-malignant HK-2 cells (Fig. 1*A*). However, the expression level of miR-141 was significantly lower in 786-O and ACHN cells compared with non-malignant HK-2 cells (Fig. 1*B*). We transiently transfected these cells with pre-miR control or pre-miR-141 (30 nM) to study the effect of miR-141 on *HOTAIR* expression. Expression of miR-141 after transient transfection is shown in Fig. 1*C*, and miR-141 significantly decreased expression of *HOTAIR* in these cells (Fig. 1*E*). In Fig. 1*D*, miR-141 expression after transfection was compared with that in HK-2 cells. A lower concentration of miR-141 (6 nM) also suppressed *HOTAIR* expression (Fig. 4*D*). These results indicate that there is a strong inverse correlation between expression of *HOTAIR* and miR-141.

Genistein (4′,5,7-trihydroxyisoflavone) is a soy isoflavone that has been reported to inhibit NF-κB and Akt signaling pathways. Genistein has been shown to induce apoptosis and cell cycle arrest and to inhibit cancer cell proliferation (29) and invasion (30). To investigate the effects of genistein on *HOTAIR* and miR-141, we treated 786-O and ACHN cells with 25 μM genistein for 96 h. Genistein treatment decreased *HOTAIR* expression and increased miR-141 expression (Fig. 1*F*), indicating that genistein had opposing effects on their expression.

Antagonistic Effect of HOTAIR and miR-141 on Cell Proliferation and Invasion—*HOTAIR* function has never been studied in renal carcinoma cells. To study the effect of *HOTAIR* on the proliferation and invasion of renal carcinoma cells, we transiently transfected 786-O and ACHN cells with siRNA control or *HOTAIR* siRNA. Transfection of *HOTAIR* siRNA decreased *HOTAIR* levels in renal carcinoma cells (Fig. 2*A*). MTS (Fig. 2*B*) and BrdU (bromodeoxyuridine) (Fig. 2*C*) assays showed that *HOTAIR* siRNA inhibited proliferation of 786-O and ACHN cells by about 40% at 96 h. These results indicate that *HOTAIR* strongly promotes cell proliferation. We also transiently transfected these cells with pre-miR control or pre-miR-141 to study the effect of miR-141 on the growth of 786-O and ACHN cells. MTS (Fig. 2*B*) and BrdU (Fig. 2*C*) assays showed that miR-141 inhibited proliferation in 786-O and ACHN cells by about 40 and 30%, respectively, at 96 h. These results indicate that miR-141 significantly inhibits cell proliferation.

DU145 prostate cancer cells have a relatively higher expression level of *HOTAIR* and miR-141 compared with non-malignant RWPE-1 prostate cells (31). miR-141 has been reported to function as a tumor suppressor in DU145 cells (32). We have also reported that *HOTAIR* promotes proliferation, reduces apoptosis, and promotes invasion in DU145 cells (33). We transiently transfected DU145 cells with anti-miR control or anti-miR-141 to study the effect of miR-141 on the growth of DU145 cells. Transient transfection of anti-miR-141 decreased miR-141 levels in DU145 cells to about 5%, and MTS (Fig. 2*D*) and BrdU (Fig. 2*E*) assays showed that anti-miR-141 increased proliferation of DU145 cells by about 20% at 96 h. These results also indicate that miR-141 inhibits DU145 cell proliferation.

Anti-miR-141 has been reported to function as an oncogene in HT-29 colorectal cancer cells (34). Therefore, we transiently transfected HT-29 cells with anti-miR control or anti-miR-141 to study the effect of miR-141 on the growth of HT-29 cells. Transient transfection of anti-miR-141 decreased miR-141 levels in HT-29 cells to about 3%, and MTS (Fig. 2*D*) and BrdU (Fig. 2*E*) assays showed that anti-miR-141 increased proliferation of HT-29 cells by about 15% at 96 h. These results also indicate that miR-141 inhibits HT-29 cell proliferation.

Because knockdown of *HOTAIR* suppressed 786-O, ACHN, and HT-29 cell proliferation, we performed apoptosis assays using flow cytometry with Annexin-V and 7-AAD. We found that *HOTAIR* siRNA increased apoptosis to about 2 times that of controls in 786-O and ACHN cells and to about 1.5 times that of controls in HT-29 cells (Fig. 2*F*), demonstrating that *HOTAIR* reduces apoptosis in these cells. We also performed apoptosis assays with miR-141-transfected cells and observed that miR-141 increased 786-O and ACHN cell apoptosis to about 3 times that of controls (Fig. 2*G*). Anti-miR-141 also reduced apoptosis about 30% compared with control in DU145 and HT-29 cells, demonstrating that miR-141 promotes apoptosis in DU145 and HT-29 cells (Fig. 2*G*).

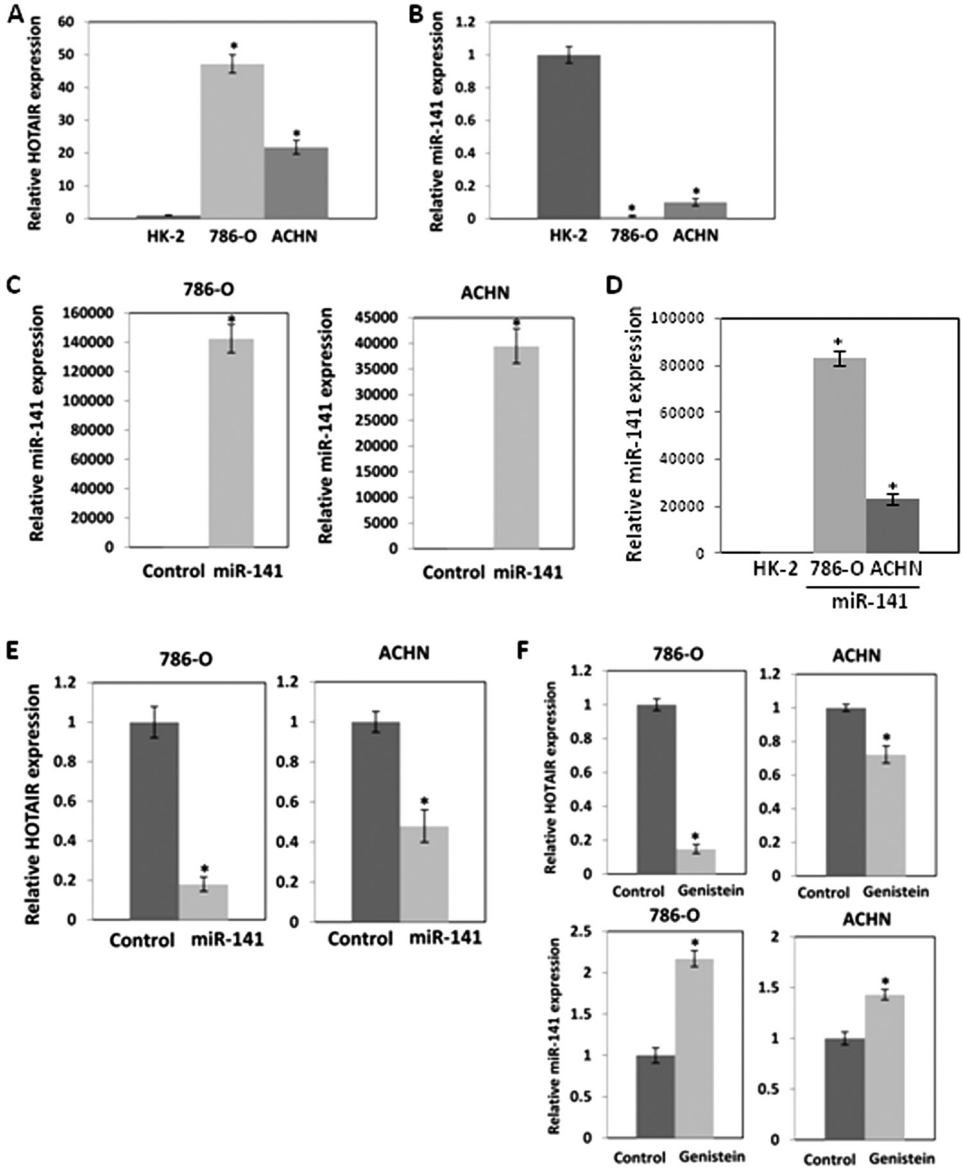

FIGURE 1. *A* and *B*, inverse expression of *HOTAIR* (*A*) and miR-141 (*B*) in renal carcinoma cells. Relative expression of *HOTAIR* and miR-141 in renal carcinoma cells was analyzed by real-time PCR and was normalized to that in non-malignant kidney HK-2 cells. Overexpression of miR-141 reduces *HOTAIR* expression in renal carcinoma cells. 786-O and ACHN cells were transfected with 30 nM pre-miR negative control or pre-miR-141 for 2 days, and miR-141 (*C*) and *HOTAIR* (*E*) expression was analyzed by real-time PCR and normalized to control. *D*, miR-141 expression after transfection was normalized to that in HK-2 cells. *F*, effect of genistein on *HOTAIR* and miR-141 expression in renal carcinoma cells. 786-O and ACHN cells were treated with 25 μM genistein for 4 days. *HOTAIR* and miR-141 expression was analyzed by real-time PCR and was normalized to that of the control. *Error bars*, S.D.

Next, we performed a transwell invasion assay using Matrigel to investigate the effect of transiently transfected *HOTAIR* siRNA on the invasive ability of 786-O and ACHN cells. The results clearly revealed that *HOTAIR* siRNA decreased cell invasion to about 40% (*HOTAIR* siRNA-1) and 50% (*HOTAIR* siRNA-2) in 786-O cells and to about 50% (*HOTAIR* siRNA-1) and 60% (*HOTAIR* siRNA-2) in ACHN cells compared with controls (Fig. 3*A*). We have previously reported that *HOTAIR* siRNA reduced DU145 cell invasion (33). We also performed a transwell invasion assay using Matrigel to investigate the effect of transiently transfected miR-141 or anti-miR-141 on the invasive ability of 786-O, ACHN, and DU145 cells. The results show that miR-141 reduced invasion of 786-O and ACHN cells to 70% and anti-miR-141 increased invasion of DU145 cells by 25% compared with controls (Fig. 3*B*). These results show the opposing effects of *HOTAIR* and miR-141 in cell proliferation and invasion.

miR-141 Binds to and Suppresses HOTAIR Expression—We examined the seed sequence of miR-141 in *HOTAIR* and found a predicted binding site for miR-141 (Fig. 4*A*). We cloned the putative miR-141 target binding sequence into a luciferase construct. Luciferase reporter assays with miR-141-overexpressing 786-O, ACHN, DU145, and HT-29 cells showed that miR-141 repressed luciferase activity. Mutation of the putative miR-141 target sites decreased the response to miR-141 (Fig. 4*B*), indicating that miR-141 binds to *HOTAIR* in a sequence-specific manner.

We also examined whether miR-141 transcriptionally suppresses *HOTAIR* because miR-141 regulates transcription factors, such as ZEB1 and ZEB2 (23, 35, 36). We treated 786-O and

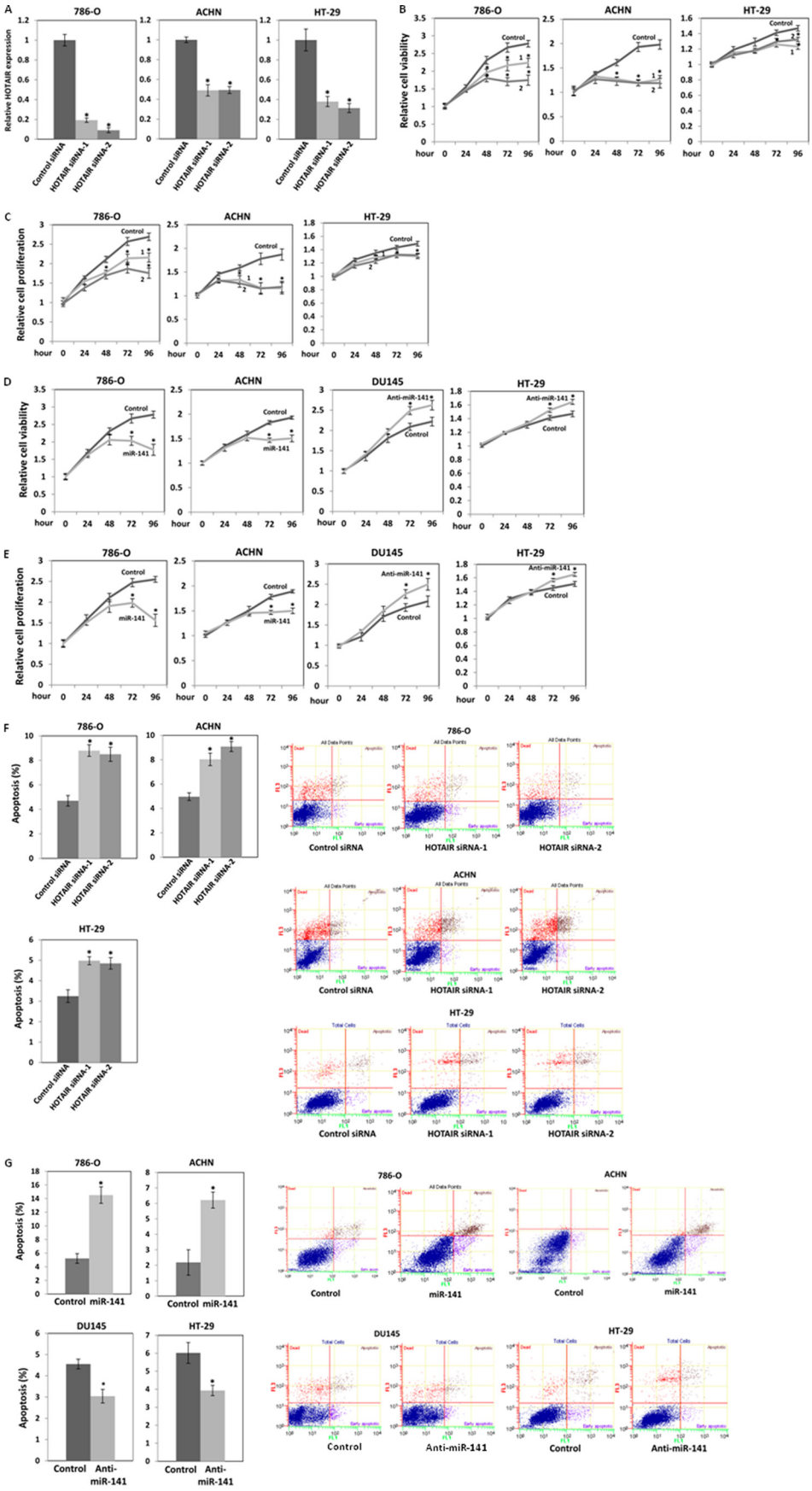
A
786-O
ACHN
HT-29
Relative HOTAIR expression
Control siRNA
HOTAIR siRNA-1
HOTAIR siRNA-2
B
Relative cell viability
Control
hour
C
Relative cell proliferation
D
DU145
Anti-miR-141
miR-141
E
F
Apoptosis (%)
G
Control miR-141
Anti-miR-141

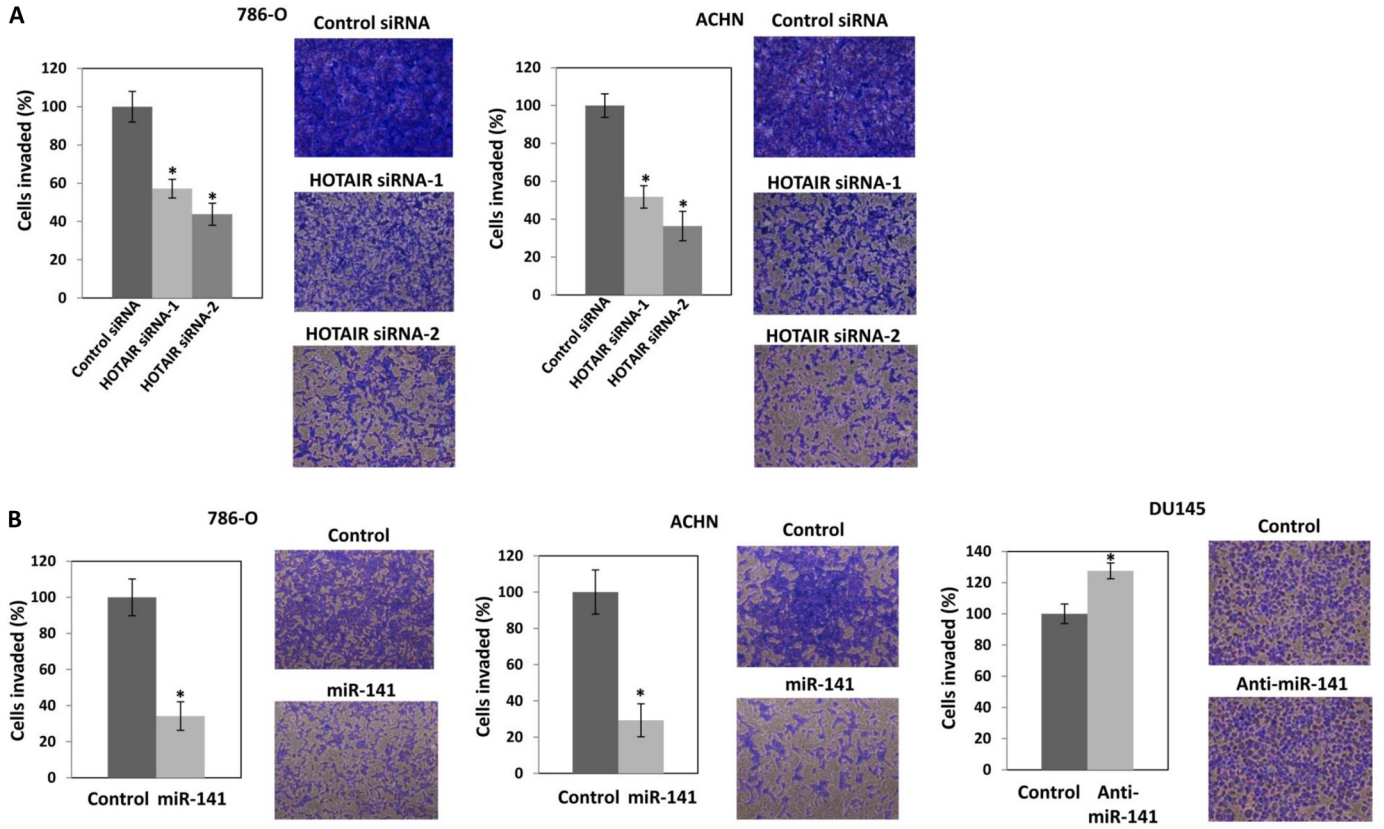

FIGURE 3. **Antagonistic effect of *HOTAIR* (*A*) and miR-141 overexpression (*B*) on cell invasion.** 786-O and ACHN cells were transiently transfected with either 30 nM siRNA control or *HOTAIR* siRNA (*A*) or 30 nM pre-miR negative control or pre-miR-141 (*B*) for 48 h. The cells were harvested and subjected to a transwell invasion assay. The values are normalized to those of control. Representative images of the invaded cells are shown on the *right*. *B*, DU145 cells were transiently transfected with 30 nM anti-miR negative control or anti-miR-141 and cell viability was assayed at the indicated times. The cells were harvested and subjected to a transwell invasion assay. The values are normalized to those of control. Representative images of the invaded cells are shown on the *right*. *Error bars*, S.D.

ACHN cells with α-amanitin, which suppresses RNA polymerase II expression and activity (37, 38) and examined *HOTAIR* expression after transfection of miR-141. α-Amanitin treatment significantly reduced RNA polymerase II expression to about 5% in both cell lines (Fig. 4*C*). However, the treatment did not significantly affect suppression of *HOTAIR* by miR-141 (Fig. 4*D*). We also measured luciferase activity with the *HOTAIR* promoter (28) in 786-O ACHN, DU145, and HT-29 cells after miR-141 transfection and found that miR-141 had no significant effect on luciferase activity (Fig. 4*E*). These results indicate that miR-141 suppresses *HOTAIR* by binding to *HOTAIR* in a sequence-specific manner and may not reduce *HOTAIR* transcription.

miR-141 Regulates HOTAIR Target Genes—*HOTAIR* has been reported to induce ABL2 and Snail and to repress PCDH10 (13). We examined mRNA (Fig. 5*A*) and protein (Fig. 5*B*) expression levels after transfection of *HOTAIR* siRNA or miR-141 to examine whether miR-141 regulates *HOTAIR* target genes. We found that *HOTAIR* siRNA and miR-141 reduced ABL2 and induced PCDH10 in 786-O cells, and we observed that *HOTAIR* siRNA-2 and miR-141 induced PCDH10 in ACHN cells. In DU145 cells, *HOTAIR* siRNA reduced Snail1, whereas anti-miR-141 induced Snail expression. In HT-29 cells, *HOTAIR* siRNA reduced ABL2 expression, whereas anti-miR-141 induced ABL2 expression. These results indicate that miR-141 regulates *HOTAIR* target genes.

Anti-miR-141 Restores HOTAIR siRNA Function—To examine if the effects of miR-141 on cell proliferation are mediated by *HOTAIR*, we co-transfected 786-O, ACHN, DU145, and HT-29 cells with *HOTAIR* siRNA and anti-miR-141 (Fig. 6*A*). Relative cell viability (Fig. 6*A*, *top*) is shown along with relative miR-141 (Fig. 6*A*, *middle*) and *HOTAIR* (Fig. 6*A*, *bottom*) expression. Anti-miR-141 transfection decreased miR-141 expression (Fig. 6*A*, *middle*, *lanes 2*, *4*, and *6* compared with *lanes 1*, *3*, and *5*), and *HOTAIR* siRNA transfection decreased

FIGURE 2. **Antagonistic effect of *HOTAIR* and miR-141 on cell proliferation.** *A*, relative *HOTAIR* expression after transient transfection of *HOTAIR* siRNA. 786-O, ACHN, and HT-29 cells were transiently transfected with 30 nM siRNA control or *HOTAIR* siRNA. *HOTAIR* expression at 48 h of the transfection was analyzed by real-time PCR and was normalized to that of the control. 786-O, ACHN, DU145, and HT-29 cells were seeded at a density of 1.5–2 × 10^3 cells/well in 96-well plates. 786-O and ACHN cells were transiently transfected with either 30 nM siRNA control or *HOTAIR* siRNA (*B* and *C*) or 30 nM pre-miR negative control or pre-miR-141 (*D* and *E*), and cell viability and proliferation were measured by MTS (*B* and *D*) and BrdU (*C* and *E*) assays at the indicated times. DU145 and HT-29 cells were transiently transfected with 30 nM anti-miR negative control or anti-miR-141, and cell viability and proliferation were measured by MTS (*D*) and BrdU (*E*). *F* and *G*, antagonistic effect of *HOTAIR* (*F*) and miR-141 (*G*) on apoptosis. 786-O and ACHN cells were transiently transfected with *HOTAIR* siRNA or pre-miR-141 as described above for 3 days. The cells were stained with Annexin-V-FITC/7-AAD, and apoptosis was analyzed by flow cytometry (*F* and *G*). HT-29 cells were transiently transfected with *HOTAIR* siRNA, and apoptosis was analyzed by flow cytometry as described above (*F*). DU145 and HT-29 cells were transiently transfected with anti-miR-141 as described above for 3 days, and apoptosis was analyzed by flow cytometry (*G*). Shown in *B* and *C* are *HOTAIR* siRNA-1 (*1*) and *HOTAIR* siRNA-2 (*2*). *Error bars*, S.D.

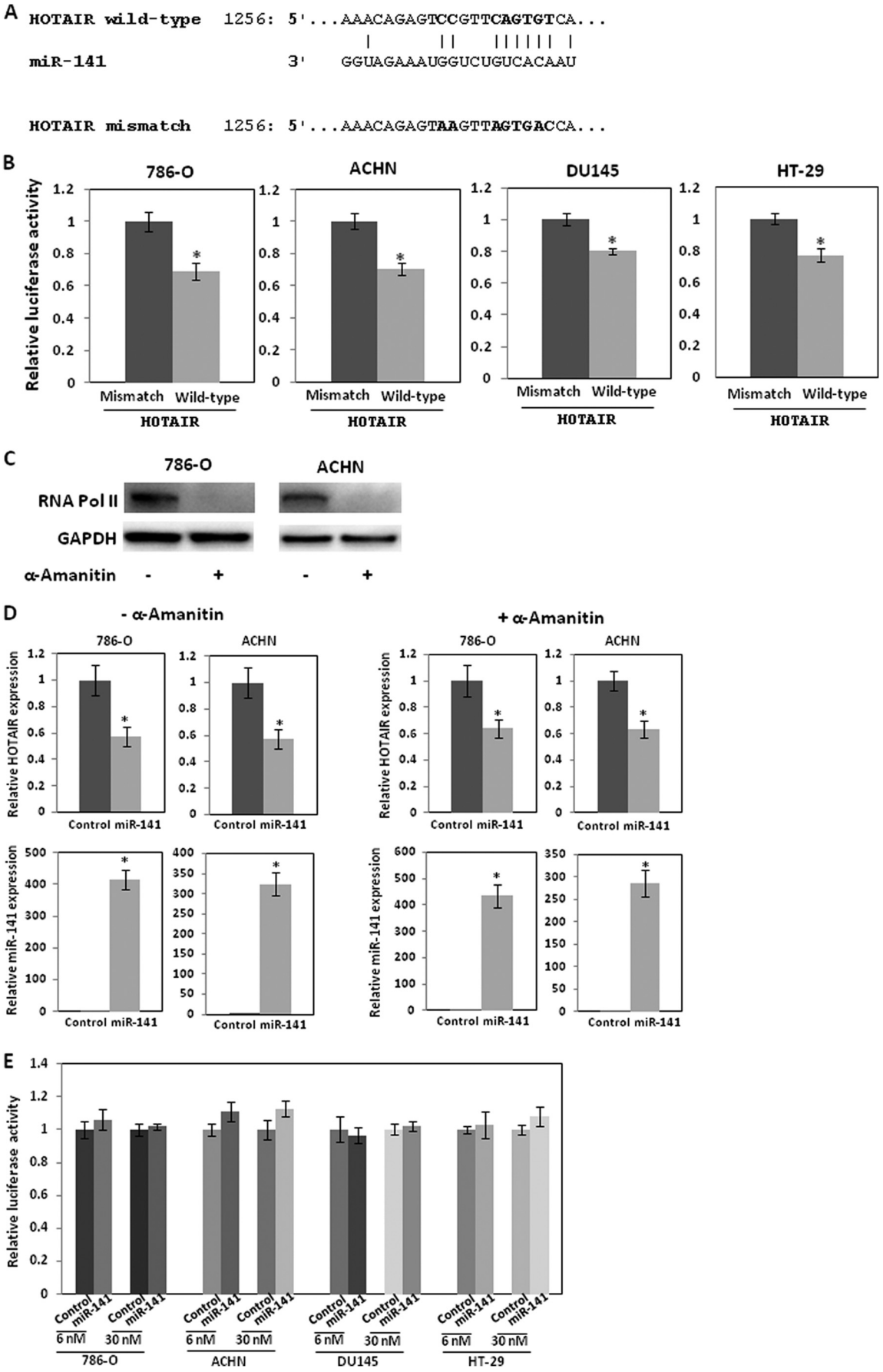
A
HOTAIR wild-type 1256: 5'...AAACAGAGTCCGTTCAGTGTCA...
miR-141 3' GGUAGAAAUGGUCUGUCACAAU
HOTAIR mismatch 1256: 5'...AAACAGAGTAAGTTAGTGACCA...
B
786-O
ACHN
DU145
HT-29
Relative luciferase activity
Mismatch
Wild-type
HOTAIR
C
786-O
ACHN
RNA Pol II
GAPDH
α-Amanitin
D
- α-Amanitin
+ α-Amanitin
Relative HOTAIR expression
Relative miR-141 expression
Control miR-141
E
Relative luciferase activity
Control miR-141
6 nM
30 nM
786-O
ACHN
DU145
HT-29

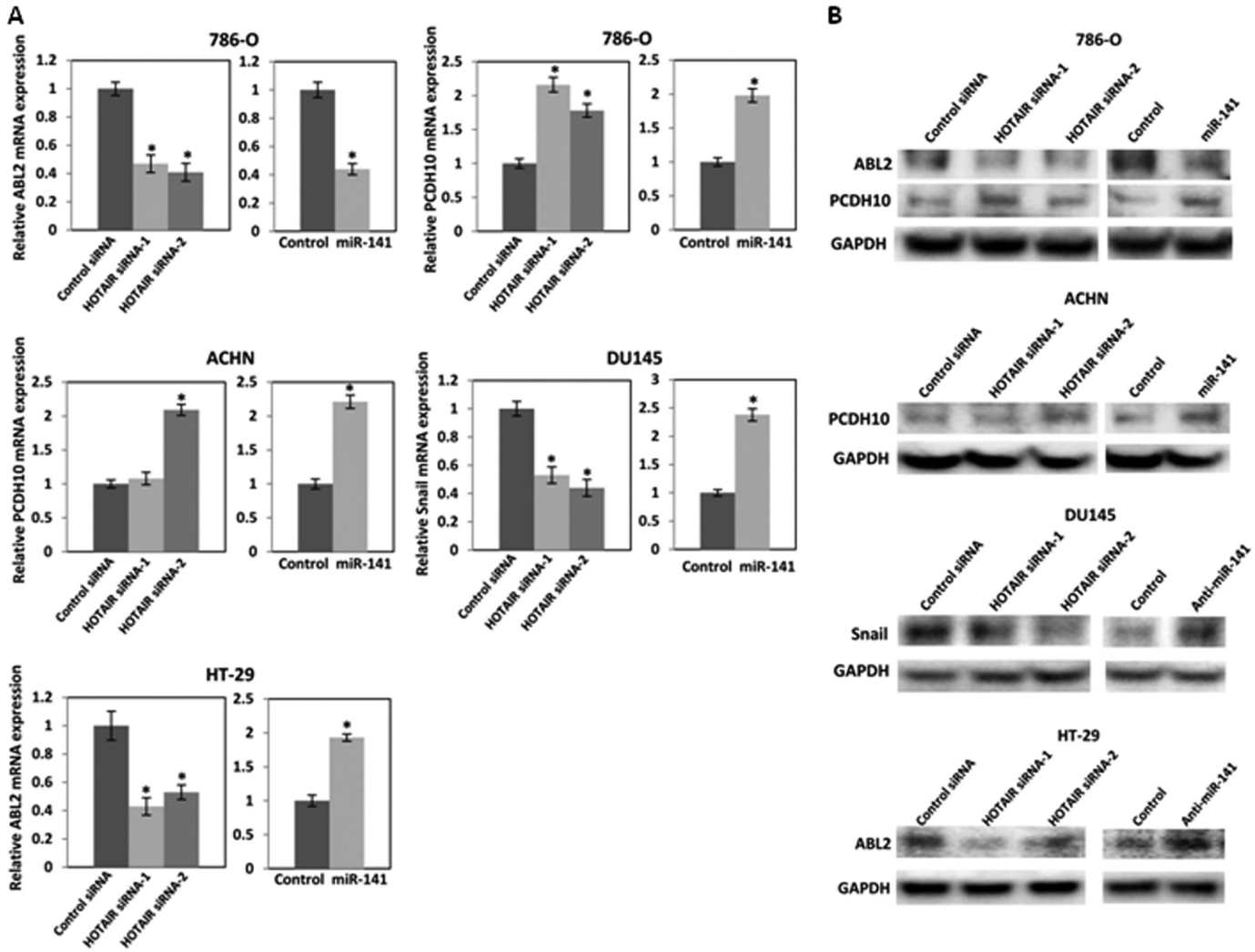

FIGURE 5. **miR-141 regulates *HOTAIR* target genes.** 786-O and ACHN cells were transfected with 30 nM control siRNA or *HOTAIR* siRNA and 30 nM pre-miR negative control or pre-miR-141. DU145 and HT-29 cells were transiently transfected with 30 nM control siRNA or *HOTAIR* siRNA and 30 nM anti-miR negative control or anti-miR-141. *A*, after a 48–72-h transfection, mRNA expression was analyzed by real-time PCR and was normalized to that of the control. *B*, after a 96-h transfection, protein expression was analyzed by Western blot. *Error bars*, S.D.

HOTAIR expression (Fig. 6*A*, *bottom*, *lanes 3–6* compared with *lane 1*). Anti-miR-141 promoted proliferation (Fig. 6*A*, *top*, *lane 2* compared with *lane 1*), and *HOTAIR* siRNA suppressed proliferation (Fig. 6*A*, *top*, *lanes 3* and *5* compared with *lane 1*). Co-transfection of anti-miR-141 and *HOTAIR* siRNA showed that *HOTAIR* siRNA suppressed the increase in cell proliferation by anti-miR-141 (Fig. 6*A*, *top*, *lanes 4* and *6* compared with *lanes 3* and *5*, respectively). Fig. 6*B* shows representative images of cells with transient co-transfection of *HOTAIR* siRNA and anti-miR-141 for 96 h. These results indicate that *HOTAIR* mediates the effects of miR-141 on cell proliferation.

We co-transfected ACHN and DU145 cells with *HOTAIR* siRNA and anti-miR-141 to study the effects of miR-141 on cell invasion mediated by *HOTAIR* (Fig. 6*C*). We observed that anti-miR-141 promoted (Fig. 6*C*, *lane 2* compared with *lane 1*) and *HOTAIR* siRNA suppressed cell invasion (Fig. 6*C*, *lanes 3* and *5* compared with *lane 1*). Co-transfection of anti-miR-141 and *HOTAIR* siRNA also showed that anti-miR-141 increased cell invasion suppressed by *HOTAIR* siRNA (Fig. 6*C*, *lanes 4* and *6* compared with *lanes 3* and *5*, respectively). Fig. 6*D* shows representative images of invaded ACHN and DU145 cells with transient co-transfection of *HOTAIR* siRNA and anti-miR-141 in the transwell invasion assay.

We also co-transfected HT-29 cells with *HOTAIR* siRNA and anti-miR-141 to study the effects of miR-141 on apoptosis mediated by *HOTAIR* (Fig. 6*E*). We observed that anti-miR-141

FIGURE 4. **miR-141 targets *HOTAIR*.** *A*, miR-141 binding sequence in *HOTAIR*. The *boldface letters* in the *HOTAIR* sequence show mutations. *B*, 786-O, ACHN DU145, and HT-29 cells in 96-well plates were transiently transfected with 30 nM pre-miR negative control or pre-miR-141 for 8 h, followed by transient transfection with 25 ng of control reporter plasmid or 3′-UTR plasmids for 48 h. 3′-UTR reporter activity was measured by a luciferase assay and normalized to the activity of *Renilla* luciferase. *C*, 786-O and ACHN cells were incubated with α-amanitin (5 μg/ml) for 15 h, and RNA polymerase II expression was analyzed by Western blot. *D*, 786-O and ACHN cells were incubated with α-amanitin (5 μg/ml) for 15 h and were transfected with 6 nM pre-miR negative control or pre-miR-141 for 2 days, and miR-141 and *HOTAIR* expression was analyzed by real-time PCR and normalized. *E*, 786-O ACHN, DU145, and HT-29 cells were transfected with 30 or 6 nM pre-miR negative control or pre-miR-141. Subsequently, the cells were transfected with pLightSwitch_Prom plasmid harboring the *HOTAIR* promoter region or pLightSwitch_Prom plasmid only, and luciferase activity was assayed 36 h after transfection. The values are normalized to controls. *Error bars*, S.D.

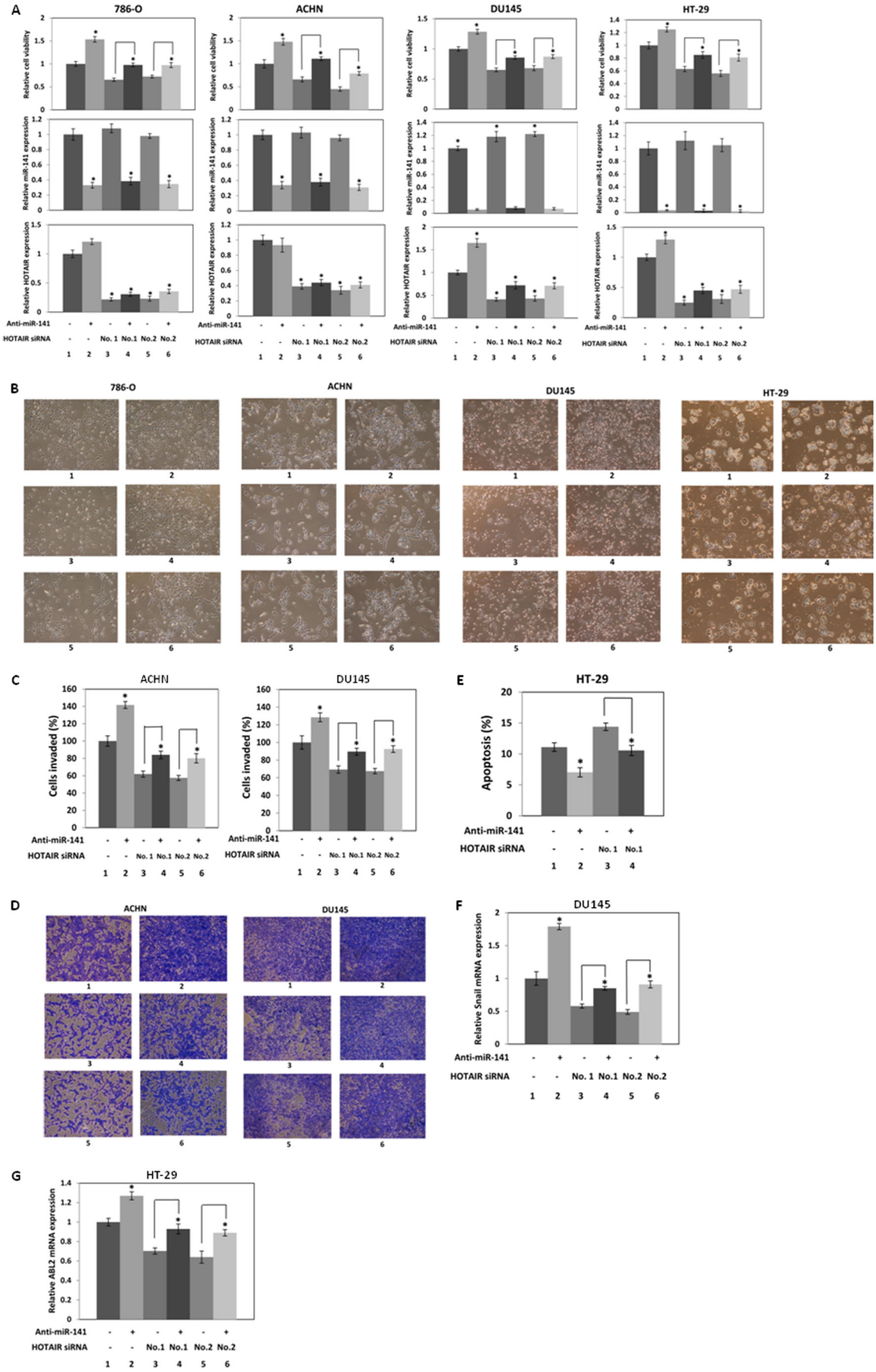
A
786-O
ACHN
DU145
HT-29
Relative cell viability
Relative miR-141 expression
Relative HOTAIR expression
Anti-miR-141
HOTAIR siRNA
No. 1
No.2
B
C
Cells invaded (%)
D
E
Apoptosis (%)
F
Relative Snail mRNA expression
G
Relative ABL2 mRNA expression

suppressed (Fig. 6*E*, *lane 2* compared with *lane 1*) and *HOTAIR* siRNA promoted apoptosis (Fig. 6*E*, *lane 3* compared with *lane 1*). Co-transfection of anti-miR-141 and *HOTAIR* siRNA also showed that anti-miR-141 suppressed the increase in apoptosis by *HOTAIR* siRNA (Fig. 6*E*, *lane 4* compared with *lane 3*).

We examined Snail expression level, which is regulated by miR-141 (Fig. 5) after co-transfection of *HOTAIR* siRNA and anti-miR-141 in DU145 cells. Anti-miR-141 induced (Fig. 6*F*, *lane 2* compared with *lane 1*) and *HOTAIR* siRNA reduced Snail (Fig. 6*F*, *lanes 3* and *5* compared with *lane 1*). Co-transfection of anti-miR-141 and *HOTAIR* siRNA showed that anti-miR-141 restored the suppression of Snail by *HOTAIR* siRNA (Fig. 6*F*, *lanes 4* and *6* compared with *lanes 3* and *5*, respectively).

We also examined ABL2 expression, which is regulated by miR-141 (Fig. 5) after co-transfection of *HOTAIR* siRNA and anti-miR-141 in HT-29 cells. Anti-miR-141 induced (Fig. 6*G*, *lane 2* compared with *lane 1*) and *HOTAIR* siRNA reduced ABL2 (Fig. 6*G*, *lanes 3* and *5* compared with *lane 1*). Co-transfection of anti-miR-141 and *HOTAIR* siRNA showed that anti-miR-141 restored the suppression of ABL2 by *HOTAIR* siRNA (Fig. 6*G*, *lanes 4* and *6* compared with *lanes 3* and *5*, respectively). Taken together, these results indicate that *HOTAIR* mediates miR-141 function in these cells.

miR-141 Suppresses HOTAIR Function—We co-transfected 786-O cells with a miR-141 binding site mutant (Fig. 4) or wild-type *HOTAIR* expression plasmid and miR-141 to investigate whether miR-141 suppresses the ectopic *HOTAIR* expression and function (Fig. 7*A*, *left*). Relative cell viability (Fig. 7*A*, *top*) is shown along with relative miR-141 (Fig. 7*A*, *middle*) and *HOTAIR* (Fig. 7*A*, *bottom*) expression. Control experiments show that miR-141 transfection increased miR-141 expression (Fig. 7*A*, *middle*, *lane 2* compared with *lane 1*), and both mutant and wild-type *HOTAIR* transfection increased *HOTAIR* expression (Fig. 7*A*, *bottom*, *lanes 3* and *5* compared with *lane 1*). miR-141 significantly decreased the ectopic wild-type *HOTAIR* expression (Fig. 7*A*, *bottom*, *lane 6* compared with *lane 5*), whereas miR-141 decreased the ectopic mutant *HOTAIR* expression about 30%. As shown previously (Fig. 2, *A* and *B*), we found that miR-141 decreased proliferation (Fig. 7*A*, *top*, *lane 2* compared with *lane 1*), whereas *HOTAIR* overexpression promoted proliferation (Fig. 7*A*, *top*, *lanes 3* and *5* compared with *lane 1*). Co-transfection of miR-141 and *HOTAIR* expression plasmid showed that miR-141 suppressed the proliferation promoted by wild-type *HOTAIR* (Fig. 7*A*, *top*, *lane 4* compared with *lane 3*) in accordance with the suppression of the ectopic wild-type *HOTAIR* expression by miR-141. These results indicate that miR-141 binds to the binding site indicated in Fig. 4; however, the mutation did not completely abolish suppression of *HOTAIR* by miR-141 (Fig. 7*A*, *bottom*, *lanes 3* and *5* compared with *lane 1*), suggesting that miR-141 also binds to other sequences in *HOTAIR*.

In ACHN cells, miR-141 transfection also increased miR-141 expression (Fig. 7*A*, *middle*, *lane 2* compared with *lane 1*), and *HOTAIR* transfection increased *HOTAIR* expression (Fig. 7*A*, *bottom*, *lane 3* compared with *lane 1*). miR-141 significantly decreased ectopic *HOTAIR* expression (Fig. 7*A*, *bottom*, *lane 4* compared with *lane 3*). We found that miR-141 decreased cell proliferation (Fig. 8*A*, *top*, *lane 2* compared with *lane 1*), whereas *HOTAIR* overexpression promoted cell proliferation (Fig. 7*A*, *top*, *lane 3* compared with *lane 1*). Co-transfection of miR-141 and *HOTAIR* expression plasmid showed that miR-141 suppressed cell proliferation promoted by *HOTAIR*. Fig. 7*B* shows representative images of renal carcinoma cells with transient co-transfection of *HOTAIR* and miR-141 for 96 h. These results indicate that miR-141 regulates *HOTAIR* in cell proliferation.

We co-transfected 786-O cells with pre-miR-141 and *HOTAIR* expression plasmid to study the effect on apoptosis (Fig. 7*C*). As shown previously (Fig. 2, *F* and *G*), miR-141 promoted apoptosis (Fig. 7*B*, *lane 2* compared with *lane 1*), whereas *HOTAIR* overexpression reduced apoptosis (Fig. 7*C*, *lane 3* compared with *lane 1*). Co-transfection of miR-141 and *HOTAIR* expression plasmid showed that miR-141 restored apoptosis inhibited by *HOTAIR* (Fig. 7*C*, *lane 4* compared with *lane 3*). Fig. 7*D* shows representative images of apoptosis with transient co-transfection of *HOTAIR* and miR-141. These results also indicate that miR-141 regulates *HOTAIR* in apoptosis.

HOTAIR Regulates miR-141 Target Gene ZEB1—miR-141 has been reported to target and repress ZEB1 (22–26). We examined ZEB1 mRNA (Fig. 8*A*) and protein (Fig. 8*B*) expression levels after transfection of *HOTAIR* siRNA or miR-141 and found that *HOTAIR* siRNA and miR-141 reduced ZEB1 expression in 786-O and ACHN cells.

We also co-transfected 786-O and ACHN cells with a miR-141 and *HOTAIR* expression plasmid miR-141 to investigate whether miR-141 suppresses ZEB1 induced by *HOTAIR*. Control experiments show that miR-141 transfection increased miR-141 expression (Fig. 8*C*, *middle*, *lane 2* compared with *lane 1*) and *HOTAIR* transfection increased *HOTAIR* expression (Fig. 8*C*, *bottom*, *lane 3* compared with *lane 1*). miR-141 significantly decreased ectopic *HOTAIR* expression (Fig. 8*C*, *bottom*, *lane 4* compared with *lane 3*). We found that miR-141 overexpression decreased ZEB1 (Fig. 8*C*, *top*, *lane 2* compared

FIGURE 6. **Anti-miR-141 restores *HOTAIR* siRNA function.** *A*, anti-miR-141 restores cell proliferation, which is suppressed by *HOTAIR* siRNA. 786-O, ACHN, and DU145 cells were co-transfected with 20 nM control siRNA or *HOTAIR* siRNA and 20 nM anti-miR negative control or anti-miR-141, and cell viability was assayed. *B*, representative images of cells transiently co-transfected with *HOTAIR* siRNA and anti-miR-141 for 96 h. *C*, anti-miR-141 restores cell invasion suppressed by *HOTAIR* siRNA. ACHN and DU145 cells were co-transfected with 20 nM control siRNA or *HOTAIR* siRNA and 20 nM anti-miR negative control or anti-miR-141 for 48 h. The cells were harvested and subjected to a transwell invasion assay. The values are normalized to those of control. *D*, representative images of invaded ACHN and DU145 cells in the transwell invasion assay. *E*, anti-miR-141 restores apoptosis suppressed by *HOTAIR* siRNA in HT-29 cells. HT-29 cells were co-transfected with 20 nM control siRNA or *HOTAIR* siRNA and 20 nM anti-miR negative control or anti-miR-141 for 72 h, and apoptosis was analyzed by flow cytometry. *F*, anti-miR-141 restores Snail mRNA level, which is suppressed by *HOTAIR* siRNA in DU145 cells. DU145 cells were co-transfected with 20 nM control siRNA or *HOTAIR* siRNA and 20 nM anti-miR negative control or anti-miR-141 for 48 h, and Snail mRNA levels were analyzed by real-time PCR and normalized to that of the control. *G*, anti-miR-141 restores ABL2 mRNA level, which is suppressed by *HOTAIR* siRNA in HT-29 cells. HT-29 cells were co-transfected with 20 nM control siRNA or *HOTAIR* siRNA and 20 nM anti-miR negative control or anti-miR-141 for 72 h, and ABL2 mRNA levels were analyzed by real-time PCR and normalized to that of the control. *A*, *B*, *C*, *D*, *F*, and *G*, control siRNA and anti-miR negative control (*1*); control siRNA and anti-miR-141 (*2*); *HOTAIR* siRNA-1 and anti-miR negative control (*3*); *HOTAIR* siRNA-1 and anti-miR-141 (*4*); *HOTAIR* siRNA-2 and anti-miR negative control (*5*); *HOTAIR* siRNA-2 and anti-miR-141 (*6*). *E*, control siRNA and anti-miR negative control (*1*); control siRNA and anti-miR-141 (*2*); *HOTAIR* siRNA-1 and anti-miR negative control (*3*); *HOTAIR* siRNA-1 and anti-miR-141 (*4*). *Error bars*, S.D.

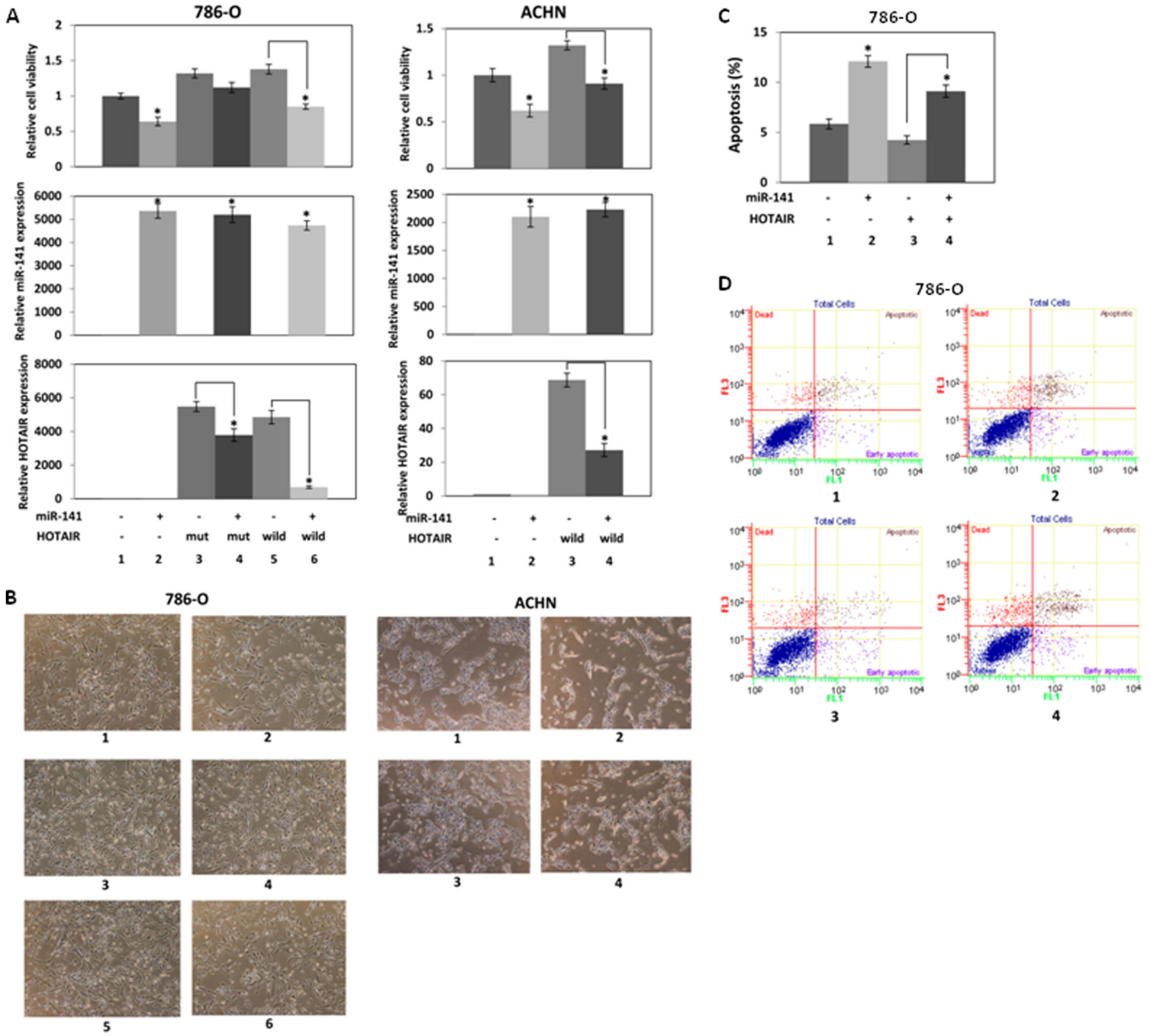

FIGURE 7. **miR-141 inhibits *HOTAIR* function.** *A*, miR-141 inhibits cell proliferation induced by *HOTAIR*. 786-O and ACHN cells in 6-well plates were co-transfected with 500 ng of control plasmid (pcDNA3.1(+)) or *HOTAIR* expression plasmid (pcDNA3.1(+)-*HOTAIR* mutant or wild type) and 30 nM pre-miR negative control or pre-miR-141, and cell viability was assayed. *Left*, for 786-O cell transfection: pcDNA3.1(+) and pre-miR negative control (*1*); pcDNA3.1(+) and pre-miR-141 (*2*); pcDNA3.1(+)-*HOTAIR* mutant and pre-miR negative control (*3*); pcDNA3.1(+)-*HOTAIR* mutant and pre-miR-141 (*4*); pcDNA3.1(+)-*HOTAIR* mutant and pre-miR negative control (*5*); pcDNA3.1(+)-*HOTAIR* mutant and pre-miR-141 (*6*). *Right*, for ACHN cell transfection: pcDNA3.1(+) and pre-miR negative control (*1*); pcDNA3.1(+) and pre-miR-141 (*2*); pcDNA3.1(+)-*HOTAIR* and pre-miR negative control (*3*); pcDNA3.1(+)-*HOTAIR* and pre-miR-141 (*4*). *B*, representative images of renal carcinoma cells with transient co-transfection of *HOTAIR* and miR-141 for 96 h. *C*, miR-141 antagonizes apoptosis, which is suppressed by *HOTAIR*. 786-O cells in 6-well plates were co-transfected with 500 ng of pcDNA3.1(+) or pcDNA3.1(+)-*HOTAIR* and 30 nM pre-miR negative control or pre-miR-141 for 72 h. The cells were stained with Annexin-V-FITC/7-AAD, and apoptosis was analyzed by flow cytometry. *1*, pcDNA3.1(+) and pre-miR negative control; *2*, pcDNA3.1(+) and pre-miR-141; *3*, pcDNA3.1(+)-*HOTAIR* and pre-miR negative control; *4*, pcDNA3.1(+)-*HOTAIR* and pre-miR-141. *D*, representative images of the apoptosis assay using flow cytometry of the transfected 786-O cells. *Error bars*, S.D.

with *lane 1*), whereas *HOTAIR* overexpression induced ZEB1 (Fig. 8*C*, *top*, *lane 3* compared with *lane 1*). Co-transfection of miR-141 and a *HOTAIR* expression plasmid showed that miR-141 suppressed ZEB1 induced by *HOTAIR* (Fig. 8*C*, *top*, *lane 4* compared with *lane 3*), suggesting that *HOTAIR* regulates the miR-141 target gene *ZEB1*.

Ago2 Mediates HOTAIR Silencing by miR-141—Ago2 is the main protein that cleaves target transcripts of miRNAs in mammalian cells (39–41). To determine whether Ago2 is responsible for silencing of *HOTAIR* by miR-141, we transfected 786-O cells with Ago2 siRNA and examined whether Ago2 siRNA reduces miR-141 silencing of endogenous *HOTAIR*. We observed that Ago2 siRNA decreased Ago2 expression (Fig. 9*A*), and miR-141 decreased endogenous *HOTAIR* expression to 20% (Fig. 9*B*, *top*). However, no significant decrease of *HOTAIR* was observed with Ago2 knockdown (Fig. 9*B*, *top*), and no significant change in miR-141 expression level was observed (Fig. 9*B*, *bottom*), suggesting that *HOTAIR* silencing largely involves Ago2.

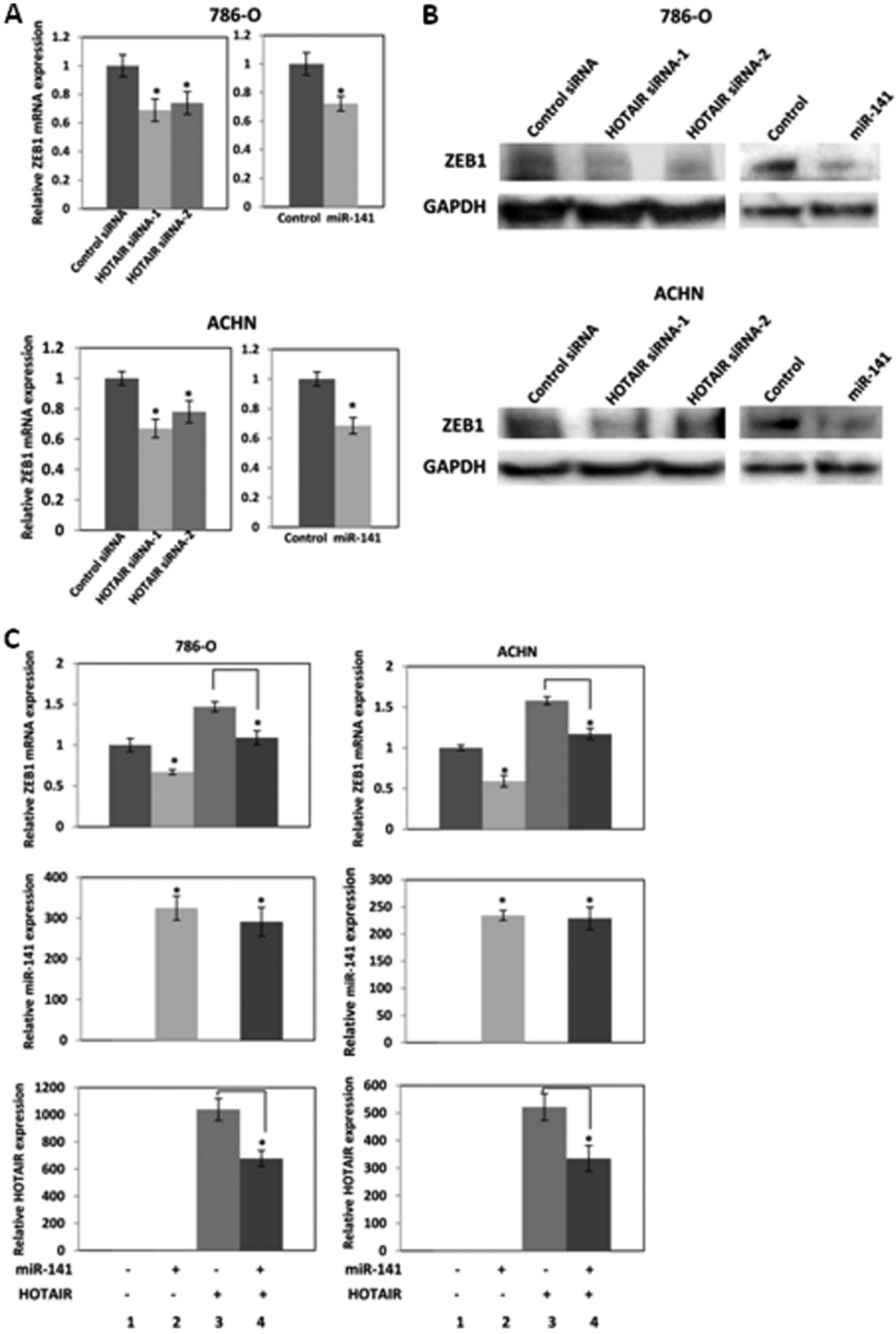
A
786-O
Relative ZEB1 mRNA expression
Control siRNA
HOTAIR siRNA-1
HOTAIR siRNA-2
Control
miR-141
ACHN
B
786-O
Control siRNA
HOTAIR siRNA-1
HOTAIR siRNA-2
Control
miR-141
ZEB1
GAPDH
ACHN
C
786-O
ACHN
Relative ZEB1 mRNA expression
Relative miR-141 expression
Relative HOTAIR expression
miR-141
HOTAIR
1
2
3
4

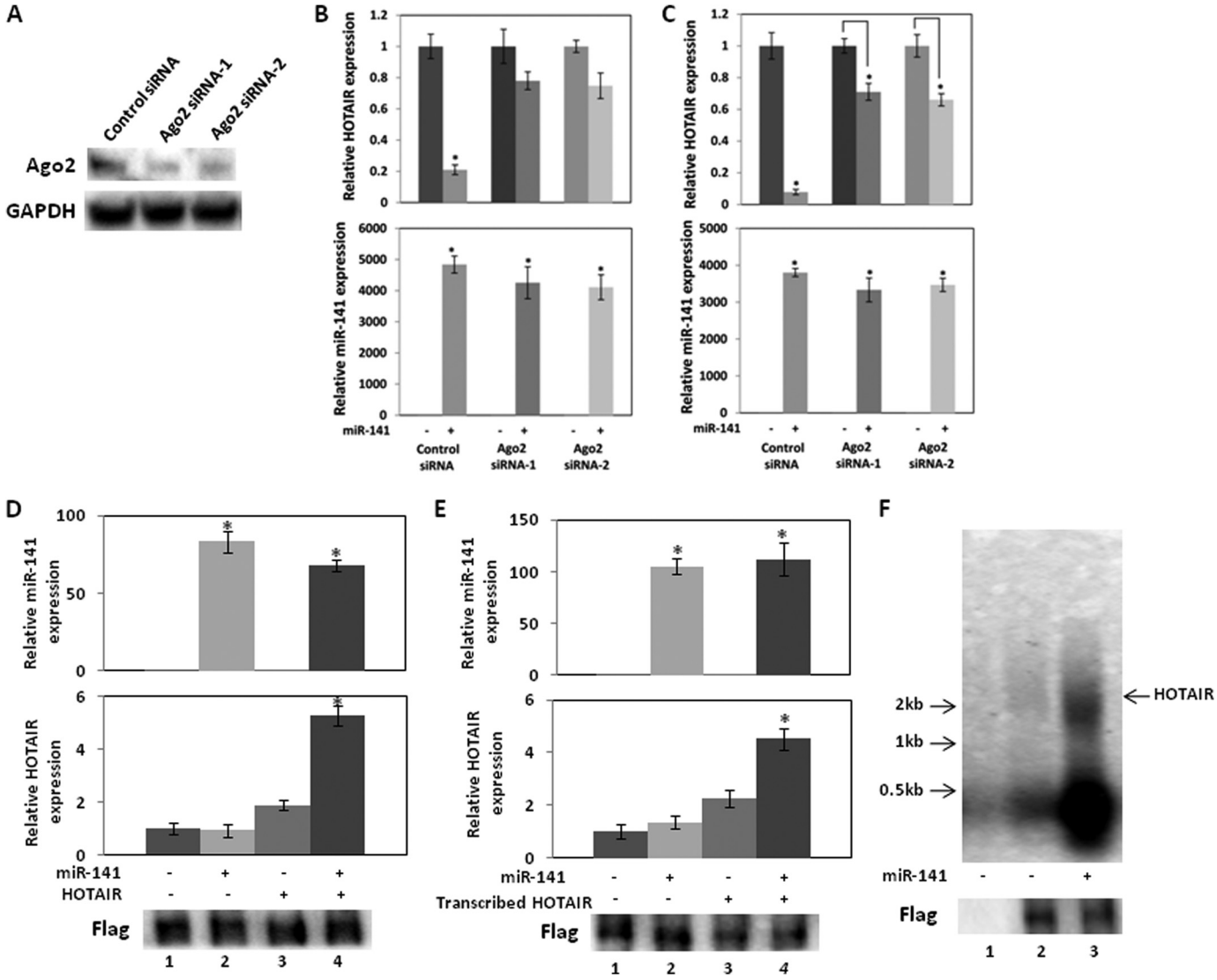

FIGURE 9. **Ago2 mediates *HOTAIR* silencing by miR-141.** *A*, Ago2 siRNA reduced Ago2 expression. 786-O cells were transiently transfected with siRNA control or one of two Ago2 siRNAs for 72 h, and Western blot analysis was performed. *B*, Ago2 knockdown reduces endogenous *HOTAIR* expression by miR-141. 786-O cells were co-transfected with 30 nM control siRNA or Ago2 siRNA and 30 nM miR negative control or miR-141. *HOTAIR* and miR-141 expression at 72 h after the transfection was analyzed by real-time PCR and normalized to that of the control. *C*, Ago2 siRNA knockdown reduces the effect of miR-141 on overexpressed *HOTAIR*. 786-O cells were co-transfected with 30 nM control siRNA or Ago2 siRNA, 30 nM miR negative control or miR-141, and a control plasmid or *HOTAIR* expression plasmid. *HOTAIR* and miR-141 expression at 72 h of the transfection was analyzed by real-time PCR and normalized to that of the control. *D*, 786-O cells in 6-well plates were co-transfected with 30 nM miR negative control or miR-141, 100 ng of control plasmid or *HOTAIR* expression plasmid, and 250 ng of FLAG-tagged Ago2 expression plasmid for 48 h, and total cell lysates were immunoprecipitated with FLAG antibody. Immunoprecipitated RNA was analyzed by real-time PCR and was normalized to that of the control. *Bottom*, Western blot of immunoprecipitated Ago2 probed by anti-FLAG antibody. *1*, pcDNA3.1(+) and pre-miR negative control; *2*, pcDNA3.1(+) and pre-miR-141; *3*, pcDNA3.1(+)-*HOTAIR* and pre-miR negative control; *4*, pcDNA3.1(+)-*HOTAIR* and pre-miR-141. FLAG-tagged Ago2 expression plasmid was transfected in *1–4*. *E*, 786-O cells in 6-well plates were co-transfected with 30 nM miR negative control or miR-141, 100 ng of control plasmid, and 250 ng of FLAG-tagged Ago2 expression plasmid for 48 h, and total cell lysates were immunoprecipitated with FLAG antibody. *In vitro* transcribed *HOTAIR* was incubated with the immunocomplex at 4 °C for 3 h. Immunoprecipitated RNA was analyzed by real-time PCR and was normalized to that of the control. *Bottom*, Western blot of immunoprecipitated Ago2 probed by anti-FLAG antibody. *1*, pre-miR negative control; *2*, pre-miR-141; *3*, purified *HOTAIR* and pre-miR negative control; *4*, purified *HOTAIR* and pre-miR-141. FLAG-tagged Ago2 expression plasmid was transfected in *1–4*. *F*, Ago2 immunocomplex cleaves *HOTAIR*. 786-O cells in 10-cm dishes were co-transfected with 30 nM miR negative control or miR-141 and 1 μg of control plasmid or FLAG-tagged Ago2 expression plasmid for 48 h, and total cell lysates were immunoprecipitated with FLAG antibody. DIG-labeled *in vitro* transcribed *HOTAIR* was incubated with immunoprecipitated Ago2 complex. After Northern blotting, DIG was probed with a DIG nucleic acid detection kit. *1*, control plasmid and pre-miR negative control; *2*, FLAG-tagged Ago2 expression plasmid and pre-miR negative control; *3*, FLAG-tagged Ago2 expression plasmid and pre-miR-141. *Error bars*, S.D.

FIGURE 8. ***HOTAIR* regulates miR-141 target gene *ZEB1*.** 786-O and ACHN cells were transfected with 30 nM control siRNA or *HOTAIR* siRNA or 6 nM pre-miR negative control or miR-141. *A*, after a 72-h transfection, *ZEB1* mRNA and *HOTAIR* expression was analyzed by real-time PCR and was normalized to that of the control. *B*, after a 96-h transfection, ZEB1 protein expression was analyzed by Western blot. *C*, miR-141 inhibits ZEB1 induced by *HOTAIR*. 786-O and ACHN cells in 6-well plates were co-transfected with 200 ng of control plasmid (pcDNA3.1(+)) or *HOTAIR* expression plasmid (pcDNA3.1(+)-*HOTAIR* mutant or wild-type) and 6 nM pre-miR negative control or pre-miR-141. After a 72-h transfection, *ZEB1* mRNA and *HOTAIR* expression was analyzed by real-time PCR and was normalized to that of the control. *1*, pcDNA3.1(+) and pre-miR negative control; *2*, pcDNA3.1(+) and pre-miR-141; *3*, pcDNA3.1(+)-*HOTAIR* and pre-miR negative control; *4*, pcDNA3.1(+)-*HOTAIR* and pre-miR-141. *Error bars*, S.D.

We also co-transfected 786-O cells with *HOTAIR* expression plasmid, miR-141, and Ago2 siRNA to investigate whether Ago2 siRNA reduces silencing of ectopic *HOTAIR* by miR-141 (Fig. 9*C*, *top*). miR-141 significantly decreased *HOTAIR* expression to 5% of control levels, whereas no significant change in miR-141 expression level was observed (Fig. 9*C*, *bottom*). With Ago2 knockdown, miR-141 reduced *HOTAIR* to only 60–70% (Fig. 9*C*, *top*) compared with controls. Thus Ago2 knockdown dramatically reduces silencing of ectopic *HOTAIR* by miR-141, suggesting that Ago2 silences *HOTAIR* in response to miR-141.

We co-transfected 786-O cells with FLAG-tagged-Ago2 and *HOTAIR* expression plasmids and miR-141 to determine if *HOTAIR* and miR-141 are present in the Ago2 immunocomplex (Fig. 9*D*). The Ago2 immunocomplex pulled down using an anti-FLAG antibody contained miR-141 or *HOTAIR* when the cells were transfected with miR-141 or *HOTAIR*. Co-transfection of miR-141 and *HOTAIR* showed an increased amount of *HOTAIR* in the immunocomplex, indicating that miR-141 recruits *HOTAIR* to the immunocomplex (Fig. 9*D*). We also investigated whether miR-141 recruits *HOTAIR* to the Ago2 immunocomplex using *in vitro* transcribed *HOTAIR*. *In vitro* transcribed *HOTAIR* was incubated with the immunocomplex. The transfection of miR-141 increased the amount of *in vitro* transcribed *HOTAIR* in the immunocomplex, indicating that miR-141 recruits *in vitro* transcribed *HOTAIR* to the immunocomplex (Fig. 9*E*). These results also suggest that miR-141 silences *HOTAIR* in an Ago2-dependent manner.

We performed cleavage assays to investigate whether Ago2 cleaves *HOTAIR* in the present of miR-141. We co-transfected 786-O cells with FLAG-tagged-Ago2 and *HOTAIR* expression plasmids with and without miR-141 and pulled-down the Ago2 immunocomplex using an anti-FLAG antibody. Incubation of *in vitro* transcribed *HOTAIR* with the Ago2 immunocomplex from cells co-transfected with miR-141 degraded *HOTAIR* into small segments (Fig. 9*F*, *lane 3*). These results indicated that *HOTAIR* is degraded and silenced by the Ago2 complex.

DISCUSSION

In this study, we have shown that *HOTAIR* is strongly and negatively regulated by miR-141 through silencing of *HOTAIR*. Interaction of miRNA with lncRNA has been reported previously. The 3′-UTR of *PTENP1*, a pseudogene of tumor suppressor gene *PTEN*, has been reported to function as a decoy of *PTEN*-targeting miRNAs (42). The lncRNA *HULC* is highly up-regulated in liver cancer and interacts with miR-372, which leads to reduced translational repression of its target gene (43). While we were preparing this manuscript, miR-21 was reported to target lncRNA *GAS5* (44). Here we have presented strong evidence that *HOTAIR* is silenced and negatively regulated by miR-141 in cancer cells.

HOTAIR is well studied among lncRNA and has been shown to have important functions in normal and cancer cells. *HOTAIR* stimulates H3K27 trimethylation to decrease expression of multiple genes through its interaction with the PRC2 (13) and promotes various types of cancers, such as breast cancer, hepatocellular carcinoma, nasopharyngeal carcinoma, and gastrointestinal stromal tumors (13–15, 45–49). However, *HOTAIR* function has never been studied in renal carcinoma cells. We found that *HOTAIR* promotes tumorigenicity in renal cell carcinoma, which is consistent with findings in other cell types. We found that *HOTAIR* and miR-141 expression are inversely correlated in renal carcinoma cells. Genistein has potent biological activity, regulates several signaling pathways in cancer cells, and promotes cancer cell death (29, 30, 50, 51), and we have found that genistein regulates miRNAs (33, 52–54). We also found that genistein decreases *HOTAIR* expression while stimulating miR-141 expression, showing an inverse effect.

Luciferase assays indicate that miR-141 reduces *HOTAIR* expression through the putative miR-141 binding site in *HOTAIR* (Fig. 4*A*). We also examined whether miR-141 alters the transcription activities on the *HOTAIR* promoter because miR-141 regulates transcription factors such as ZEB1 and ZEB2 (23, 35, 36). Treatment with α-amanitin, an inhibitor of RNA polymerase II, did not significantly affect miR-141 suppression of *HOTAIR* in 786-O and ACHN cells (Fig. 4, *C* and *D*), and miR-141 also did not have significant effects on luciferase activity using a *HOTAIR* promoter (Fig. 4*D*). These results demonstrate that miR-141 did not transcriptionally repress *HOTAIR*. Our results show that miR-141 significantly targets and suppresses *HOTAIR* through the putative binding site, although we cannot exclude the possibility of transcriptionally suppression or other unknown mechanisms.

Functional analyses with co-transfection of *HOTAIR* siRNA or a *HOTAIR* expression plasmid and miR-141 or anti-miR-141 clearly show that miR-141 suppressed *HOTAIR* expression and function and that miR-141 function is mediated by *HOTAIR*. miR-141 significantly repressed wild-type *HOTAIR*, but a mutated putative *HOTAIR* binding site (Fig. 4) did not completely abolish the repression by miR-141 (Fig. 8), suggesting that miR-141 may bind to other sequences in *HOTAIR*.

HOTAIR has been reported to induce ABL2, Snail, LAMB3, and LAMC2 and repress JAM2, PCDH10, and MDA-MB-231 cells (13). We found that *HOTAIR* siRNA and miR-141 reduced ABL2 and induced PCDH10 in 786-O cells, and we observed that *HOTAIR* siRNA and miR-141 induced PCDH10 in ACHN cells. The difference in effects on *HOTAIR* target genes may be due to the difference in 786-O and ACHN cell type. 786-O cells are derived from a primary clear cell adenocarcinoma, and ACHN cells are derived from a metastatic renal adenocarcinoma. 786-O cells contain loss of heterozygosity of the *VHL* (von Hippel-Lindau) tumor suppressor, whereas ACHN cells harbor wild-type *VHL*. *HOTAIR* was found to regulate the miR-141 target gene ZEB1 in both 786-O and ACHN cells. *HOTAIR* siRNA reduced Snail1, whereas anti-miR-141 induced Snail expression in DU145 prostate cancer cells. *HOTAIR* siRNA reduced ABL2, whereas anti-miR-141 induced ABL2 expression in HT-29 colorectal adenocarcinoma cells. miR-141 may regulate these genes, which regulate metastasis and invasion, and the results of the co-transfection assays support the conclusion that miR-141 regulate genes by targeting *HOTAIR*.

miRNAs guide complementary target mRNAs to the RNA-induced silencing complex that contains Argonaute family proteins. Ago2 is the main protein that cleaves target transcripts directly in mammalian cells (39–41). In this study, an Ago2 siRNA was found to prevent the decrease in *HOTAIR* expression by miR-141. *HOTAIR* and miR-141 were both found to be

present in the Ago2 immunocomplex. Cleavage experiments show that *HOTAIR* is degraded into small segments in the presence of miR-141 (Fig. 9*F*). Thus, we have conclusively shown that miR-141 targets and cleaves *HOTAIR* in an Ago2-dependent manner similar to that by which miRNAs cause degradation of protein-coding mRNAs. However, our results do not exclude other mechanisms of lncRNA silencing by miRNAs.

Mammalian miRNA target sites are primarily in the 3′-UTR of mRNA transcripts, whereas most plant miRNAs target mRNA protein-coding regions. Studies have indicated that miRNA targets in protein-coding sequences regulate target genes (55–58), and genome-wide analysis demonstrated that a large number of Ago binding sites are located in human protein-coding regions (59, 60). However, it is believed that active mRNA translation interrupts miRNA from binding to its target site in a protein-coding region (61, 62). It has also been demonstrated that 3′ UTR sites are more effective in down-regulating gene expression than sites located in the protein-coding region (55, 60, 61). Because lncRNAs are not utilized for mRNA translation, its target sequence is readily accessible to miRNAs, as is the 3′-UTR of mRNA targeted by miRNAs. It is believed that a number of lncRNAs may be targets of miRNAs.

lncRNAs and miRNAs are essential regulators of gene expression, and it has been documented that these non-coding RNAs play important roles in diverse biological processes, such as development and disease. Interaction between lncRNA and miRNA provides another element of control in gene regulation. These results have provided strong evidence that shows that miR-141 targets and silences *HOTAIR* in an Ago2-dependent manner and regulates its function. They suggest that broad spectrum silencing by RNA interaction significantly regulates gene expression and cellular functions.

Acknowledgment—We thank Dr. Roger Erickson for support and assistance with the preparation of the manuscript.

REFERENCES

1. Bertone, P., Stolc, V., Royce, T. E., Rozowsky, J. S., Urban, A. E., Zhu, X., Rinn, J. L., Tongprasit, W., Samanta, M., Weissman, S., Gerstein, M., and Snyder, M. (2004) Global identification of human transcribed sequences with genome tiling arrays. *Science* **306,** 2242–2246
2. Kapranov, P., Cawley, S. E., Drenkow, J., Bekiranov, S., Strausberg, R. L., Fodor, S. P., and Gingeras, T. R. (2002) Large-scale transcriptional activity in chromosomes 21 and 22. *Science* **296,** 916–919
3. Rinn, J. L., Euskirchen, G., Bertone, P., Martone, R., Luscombe, N. M., Hartman, S., Harrison, P. M., Nelson, F. K., Miller, P., Gerstein, M., Weissman, S., and Snyder, M. (2003) The transcriptional activity of human chromosome 22. *Genes Dev.* **17,** 529–540
4. Rinn, J. L., Kertesz, M., Wang, J. K., Squazzo, S. L., Xu, X., Brugmann, S. A., Goodnough, L. H., Helms, J. A., Farnham, P. J., Segal, E., and Chang, H. Y. (2007) Functional demarcation of active and silent chromatin domains in human HOX loci by noncoding RNAs. *Cell* **129,** 1311–1323
5. Huarte, M., and Rinn, J. L. (2010) Large non-coding RNAs: missing links in cancer? *Hum. Mol. Genet.* **19,** R152–R161
6. Esteller, M. (2011) Non-coding RNAs in human disease. *Nat. Rev. Genet.* **12,** 861–874
7. Wang, K. C., and Chang, H. Y. (2011) Molecular mechanisms of long noncoding RNAs. *Mol. Cell* **43,** 904–914
8. Khalil, A. M., Guttman, M., Huarte, M., Garber, M., Raj, A., Rivea Morales, D., Thomas, K., Presser, A., Bernstein, B. E., van Oudenaarden, A., Regev, A., Lander, E. S., and Rinn, J. L. (2009) Many human large intergenic noncoding RNAs associate with chromatin-modifying complexes and affect gene expression. *Proc. Natl. Acad. Sci. U.S.A.* **106,** 11667–11672
9. Wang, K. C., Yang, Y. W., Liu, B., Sanyal, A., Corces-Zimmerman, R., Chen, Y., Lajoie, B. R., Protacio, A., Flynn, R. A., Gupta, R. A., Wysocka, J., Lei, M., Dekker, J., Helms, J. A., and Chang, H. Y. (2011) A long noncoding RNA maintains active chromatin to coordinate homeotic gene expression. *Nature* **472,** 120–124
10. Guttman, M., Amit, I., Garber, M., French, C., Lin, M. F., Feldser, D., Huarte, M., Zuk, O., Carey, B. W., Cassady, J. P., Cabili, M. N., Jaenisch, R., Mikkelsen, T. S., Jacks, T., Hacohen, N., Bernstein, B. E., Kellis, M., Regev, A., Rinn, J. L., and Lander, E. S. (2009) Chromatin signature reveals over a thousand highly conserved large non-coding RNAs in mammals. *Nature* **458,** 223–227
11. Tsai, M. C., Manor, O., Wan, Y., Mosammaparast, N., Wang, J. K., Lan, F., Shi, Y., Segal, E., and Chang, H. Y. (2010) Long noncoding RNA as modular scaffold of histone modification complexes. *Science* **329,** 689–693
12. Guttman, M., Donaghey, J., Carey, B. W., Garber, M., Grenier, J. K., Munson, G., Young, G., Lucas, A. B., Ach, R., Bruhn, L., Yang, X., Amit, I., Meissner, A., Regev, A., Rinn, J. L., Root, D. E., and Lander, E. S. (2011) lincRNAs act in the circuitry controlling pluripotency and differentiation. *Nature* **477,** 295–300
13. Gupta, R. A., Shah, N., Wang, K. C., Kim, J., Horlings, H. M., Wong, D. J., Tsai, M. C., Hung, T., Argani, P., Rinn, J. L., Wang, Y., Brzoska, P., Kong, B., Li, R., West, R. B., van de Vijver, M. J., Sukumar, S., and Chang, H. Y. (2010) Long non-coding RNA HOTAIR reprograms chromatin state to promote cancer metastasis. *Nature* **464,** 1071–1076
14. Kogo, R., Shimamura, T., Mimori, K., Kawahara, K., Imoto, S., Sudo, T., Tanaka, F., Shibata, K., Suzuki, A., Komune, S., Miyano, S., and Mori, M. (2011) Long noncoding RNA HOTAIR regulates polycomb-dependent chromatin modification and is associated with poor prognosis in colorectal cancers. *Cancer Res.* **71,** 6320–6326
15. Kim, K., Jutooru, I., Chadalapaka, G., Johnson, G., Frank, J., Burghardt, R., Kim, S., and Safe, S. (2013) HOTAIR is a negative prognostic factor and exhibits pro-oncogenic activity in pancreatic cancer. *Oncogene* **32,** 1616–1625
16. Bartel, D. P. (2009) MicroRNAs: target recognition and regulatory functions. *Cell* **136,** 215–233
17. Fabian, M. R., and Sonenberg, N. (2012) The mechanics of miRNA-mediated gene silencing: a look under the hood of miRISC. *Nat. Struct. Mol. Biol.* **19,** 586–593
18. Friedman, R. C., Farh, K. K., Burge, C. B., and Bartel, D. P. (2009) Most mammalian mRNAs are conserved targets of microRNAs. *Genome Res.* **19,** 92–105
19. Lewis, B. P., Burge, C. B., and Bartel, D. P. (2005) Conserved seed pairing, often flanked by adenosines, indicates that thousands of human genes are microRNA targets. *Cell* **120,** 15–20
20. Croce, C. M. (2009) Causes and consequences of microRNA dysregulation in cancer. *Nat. Rev. Genet.* **10,** 704–714
21. Kent, O. A., and Mendell, J. T. (2006) A small piece in the cancer puzzle: microRNAs as tumor suppressors and oncogenes. *Oncogene* **25,** 6188–6196
22. Park, S. M., Gaur, A. B., Lengyel, E., and Peter, M. E. (2008) The miR-200 family determines the epithelial phenotype of cancer cells by targeting the E-cadherin repressors ZEB1 and ZEB2. *Genes Dev.* **22,** 894–907
23. Gregory, P. A., Bert, A. G., Paterson, E. L., Barry, S. C., Tsykin, A., Farshid, G., Vadas, M. A., Khew-Goodall, Y., and Goodall, G. J. (2008) The miR-200 family and miR-205 regulate epithelial to mesenchymal transition by targeting ZEB1 and SIP1. *Nat. Cell Biol.* **10,** 593–601
24. Korpal, M., Lee, E. S., Hu, G., and Kang, Y. (2008) The miR-200 family inhibits epithelial-mesenchymal transition and cancer cell migration by direct targeting of E-cadherin transcriptional repressors ZEB1 and ZEB2. *J. Biol. Chem.* **283,** 14910–14914
25. Bracken, C. P., Gregory, P. A., Kolesnikoff, N., Bert, A. G., Wang, J., Shannon, M. F., and Goodall, G. J. (2008) A double-negative feedback loop between ZEB1-SIP1 and the microRNA-200 family regulates epithelial-mesenchymal transition. *Cancer Res.* **68,** 7846–7854
26. Korpal, M., Ell, B. J., Buffa, F. M., Ibrahim, T., Blanco, M. A., Celià-Terrassa, T., Mercatali, L., Khan, Z., Goodarzi, H., Hua, Y., Wei, Y., Hu, G., Garcia, B. A., Ragoussis, J., Amadori, D., Harris, A. L., and Kang, Y. (2011)

Direct targeting of Sec23a by miR-200s influences cancer cell secretome and promotes metastatic colonization. *Nat. Med.* **17,** 1101–1108
27. Landthaler, M., Gaidatzis, D., Rothballer, A., Chen, P. Y., Soll, S. J., Dinic, L., Ojo, T., Hafner, M., Zavolan, M., and Tuschl, T. (2008) Molecular characterization of human Argonaute-containing ribonucleoprotein complexes and their bound target mRNAs. *RNA* **14,** 2580–2596
28. Bhan, A., Hussain, I., Ansari, K. I., Kasiri, S., Bashyal, A., and Mandal, S. S. (2013) Antisense transcript long noncoding RNA (lncRNA) HOTAIR is transcriptionally induced by estradiol. *J. Mol. Biol.* **425,** 3707–3722
29. Banerjee, S., Li, Y., Wang, Z., and Sarkar, F. H. (2008) Multi-targeted therapy of cancer by genistein. *Cancer Lett.* **269,** 226–242
30. Pavese, J. M., Farmer, R. L., and Bergan, R. C. (2010) Inhibition of cancer cell invasion and metastasis by genistein. *Cancer Metastasis Rev.* **29,** 465–482
31. Xiao, J., Gong, A. Y., Eischeid, A. N., Chen, D., Deng, C., Young, C. Y., and Chen, X. M. (2012) miR-141 modulates androgen receptor transcriptional activity in human prostate cancer cells through targeting the small heterodimer partner protein. *Prostate* **72,** 1514–1522
32. Liu, C. (2012) *MicroRNA Regulation of Prostate Cancer Stem/Progenitor Cells and Prostate Cancer Development*, Ph.D. dissertation, University of Texas Health Science Center, Houston, TX
33. Chiyomaru, T., Yamamura, S., Fukuhara, S., Hidaka, H., Majid, S., Saini, S., Arora, S., Deng, G., Shahryari, V., Chang, I., Tanaka, Y., Tabatabai, Z. L., Enokida, H., Seki, N., Nakagawa, M., and Dahiya, R. (2013) Genistein up-regulates tumor suppressor microRNA-574–3p in prostate cancer. *PloS One* **8,** e58929
34. Hu, M., Xia, M., Chen, X., Lin, Z., Xu, Y., Ma, Y., and Su, L. (2010) MicroRNA-141 regulates Smad interacting protein 1 (SIP1) and inhibits migration and invasion of colorectal cancer cells. *Dig. Dis. Sci.* **55,** 2365–2372
35. Nakada, C., Matsuura, K., Tsukamoto, Y., Tanigawa, M., Yoshimoto, T., Narimatsu, T., Nguyen, L. T., Hijiya, N., Uchida, T., Sato, F., Mimata, H., Seto, M., and Moriyama, M. (2008) Genome-wide microRNA expression profiling in renal cell carcinoma: significant down-regulation of miR-141 and miR-200c. *J. Pathol.* **216,** 418–427
36. Xu, H., Mei, Q., Xiong, C., and Zhao, J. (2013) Tumor-suppressing effects of miR-141 in human osteosarcoma. *Cell Biochem. Biophys.*, in press
37. Gong, X. Q., Nedialkov, Y. A., and Burton, Z. F. (2004) α-Amanitin blocks translocation by human RNA polymerase II. *J. Biol. Chem.* **279,** 27422–27427
38. Nguyen, V. T., Giannoni, F., Dubois, M. F., Seo, S. J., Vigneron, M., Kédinger, C., and Bensaude, O. (1996) *In vivo* degradation of RNA polymerase II largest subunit triggered by α-amanitin. *Nucleic Acids Res.* **24,** 2924–2929
39. Liu, J., Carmell, M. A., Rivas, F. V., Marsden, C. G., Thomson, J. M., Song, J. J., Hammond, S. M., Joshua-Tor, L., and Hannon, G. J. (2004) Argonaute2 is the catalytic engine of mammalian RNAi. *Science* **305,** 1437–1441
40. Hutvagner, G., and Simard, M. J. (2008) Argonaute proteins: key players in RNA silencing. *Nat. Rev. Mol. Cell Biol.* **9,** 22–32
41. Pratt, A. J., and MacRae, I. J. (2009) The RNA-induced silencing complex: a versatile gene-silencing machine. *J. Biol. Chem.* **284,** 17897–17901
42. Poliseno, L., Salmena, L., Zhang, J., Carver, B., Haveman, W. J., and Pandolfi, P. P. (2010) A coding-independent function of gene and pseudogene mRNAs regulates tumour biology. *Nature* **465,** 1033–1038
43. Wang, J., Liu, X., Wu, H., Ni, P., Gu, Z., Qiao, Y., Chen, N., Sun, F., and Fan, Q. (2010) CREB up-regulates long non-coding RNA, HULC expression through interaction with microRNA-372 in liver cancer. *Nucleic Acids Res.* **38,** 5366–5383
44. Zhang, Z., Zhu, Z., Watabe, K., Zhang, X., Bai, C., Xu, M., Wu, F., and Mo, Y. Y. (2013) Negative regulation of lncRNA GAS5 by miR-21. *Cell Death Differ.* **20,** 1558–1568
45. Bhan, A., Hussain, I., Ansari, K. I., Kasiri, S., Bashyal, A., and Mandal, S. S. (2013) Antisense transcript long noncoding RNA (lncRNA) HOTAIR is transcriptionally induced by estradiol. *J. Mol. Biol.* **425,** 3707–3722
46. Ishibashi, M., Kogo, R., Shibata, K., Sawada, G., Takahashi, Y., Kurashige, J., Akiyoshi, S., Sasaki, S., Iwaya, T., Sudo, T., Sugimachi, K., Mimori, K., Wakabayashi, G., and Mori, M. (2013) Clinical significance of the expression of long non-coding RNA HOTAIR in primary hepatocellular carcinoma. *Oncol. Rep.* **29,** 946–950
47. Nie, Y., Liu, X., Qu, S., Song, E., Zou, H., and Gong, C. (2013) Long non-coding RNA HOTAIR is an independent prognostic marker for nasopharyngeal carcinoma progression and survival. *Cancer Sci.* **104,** 458–464
48. Lu, L., Zhu, G., Zhang, C., Deng, Q., Katsaros, D., Mayne, S. T., Risch, H. A., Mu, L., Canuto, E. M., Gregori, G., Benedetto, C., and Yu, H. (2012) Association of large noncoding RNA HOTAIR expression and its downstream intergenic CpG island methylation with survival in breast cancer. *Breast Cancer Res. Treat.* **136,** 875–883
49. Niinuma, T., Suzuki, H., Nojima, M., Nosho, K., Yamamoto, H., Takamaru, H., Yamamoto, E., Maruyama, R., Nobuoka, T., Miyazaki, Y., Nishida, T., Bamba, T., Kanda, T., Ajioka, Y., Taguchi, T., Okahara, S., Takahashi, H., Nishida, Y., Hosokawa, M., Hasegawa, T., Tokino, T., Hirata, K., Imai, K., Toyota, M., and Shinomura, Y. (2012) Upregulation of miR-196a and HOTAIR drive malignant character in gastrointestinal stromal tumors. *Cancer Res.* **72,** 1126–1136
50. Zhang, Y., and Chen, H. (2011) Genistein, an epigenome modifier during cancer prevention. *Epigenetics* **6,** 888–891
51. Zhang, Y., and Chen, H. (2011) Genistein attenuates WNT signaling by up-regulating sFRP2 in a human colon cancer cell line. *Exp. Biol. Med.* (*Maywood*) **236,** 714–722
52. Chiyomaru, T., Yamamura, S., Fukuhara, S., Yoshino, H., Kinoshita, T., Majid, S., Saini, S., Chang, I., Tanaka, Y., Enokida, H., Seki, N., Nakagawa, M., and Dahiya, R. (2013) Genistein inhibits prostate cancer cell growth by targeting miR-34a and oncogenic HOTAIR. *PloS One* **8,** e70372
53. Chiyomaru, T., Yamamura, S., Zaman, M. S., Majid, S., Deng, G., Shahryari, V., Saini, S., Hirata, H., Ueno, K., Chang, I., Tanaka, Y., Tabatabai, Z. L., Enokida, H., Nakagawa, M., and Dahiya, R. (2012) Genistein suppresses prostate cancer growth through inhibition of oncogenic microRNA-151. *PloS One* **7,** e43812
54. Majid, S., Dar, A. A., Saini, S., Chen, Y., Shahryari, V., Liu, J., Zaman, M. S., Hirata, H., Yamamura, S., Ueno, K., Tanaka, Y., and Dahiya, R. (2010) Regulation of minichromosome maintenance gene family by microRNA-1296 and genistein in prostate cancer. *Cancer Res.* **70,** 2809–2818
55. Forman, J. J., Legesse-Miller, A., and Coller, H. A. (2008) A search for conserved sequences in coding regions reveals that the let-7 microRNA targets Dicer within its coding sequence. *Proc. Natl. Acad. Sci. U.S.A.* **105,** 14879–14884
56. Schnall-Levin, M., Rissland, O. S., Johnston, W. K., Perrimon, N., Bartel, D. P., and Berger, B. (2011) Unusually effective microRNA targeting within repeat-rich coding regions of mammalian mRNAs. *Genome Res.* **21,** 1395–1403
57. Schnall-Levin, M., Zhao, Y., Perrimon, N., and Berger, B. (2010) Conserved microRNA targeting in *Drosophila* is as widespread in coding regions as in 3′UTRs. *Proc. Natl. Acad. Sci. U.S.A.* **107,** 15751–15756
58. Tay, Y., Zhang, J., Thomson, A. M., Lim, B., and Rigoutsos, I. (2008) MicroRNAs to Nanog, Oct4 and Sox2 coding regions modulate embryonic stem cell differentiation. *Nature* **455,** 1124–1128
59. Chi, S. W., Zang, J. B., Mele, A., and Darnell, R. B. (2009) Argonaute HITS-CLIP decodes microRNA-mRNA interaction maps. *Nature* **460,** 479–486
60. Hafner, M., Landthaler, M., Burger, L., Khorshid, M., Hausser, J., Berninger, P., Rothballer, A., Ascano, M., Jr., Jungkamp, A. C., Munschauer, M., Ulrich, A., Wardle, G. S., Dewell, S., Zavolan, M., and Tuschl, T. (2010) Transcriptome-wide identification of RNA-binding protein and microRNA target sites by PAR-CLIP. *Cell* **141,** 129–141
61. Gu, S., Jin, L., Zhang, F., Sarnow, P., and Kay, M. A. (2009) Biological basis for restriction of microRNA targets to the 3′ untranslated region in mammalian mRNAs. *Nat. Struct. Mol. Biol.* **16,** 144–150
62. Lin, H. R., and Ganem, D. (2011) Viral microRNA target allows insight into the role of translation in governing microRNA target accessibility. *Proc. Natl. Acad. Sci. U.S.A.* **108,** 5148–5153